

UNIVERSITÉ DU QUÉBEC EN ABITIBI-TÉMISCAMINGUE

ÉCOLE DE GÉNIE

ÉTUDE ET POSITIONNEMENT UTILISANT LE RESEAU DE CAPTEURS SANS
FIL DANS UN ENVIRONNEMENT MINIER SOUTERRAIN

TRACKING AND POSITIONING IN THE UNDERGROUND MINE USING
WIRELESS SENSOR NETWORK (WSN)

MÉMOIRE

PRÉSENTÉ

COMME EXIGENCE PARTIELLE

DE LA MAÎTRISE EN INGÉNIERIE

PAR

BIKI BARUA

OCTOBRE 2017



BIBLIOTHÈQUE

Cégep de l'Abitibi-Témiscamingue
Université du Québec en Abitibi-Témiscamingue

Mise en garde

La bibliothèque du Cégep de l'Abitibi-Témiscamingue et de l'Université du Québec en Abitibi-Témiscamingue a obtenu l'autorisation de l'auteur de ce document afin de diffuser, dans un but non lucratif, une copie de son œuvre dans Depositum, site d'archives numériques, gratuit et accessible à tous.

L'auteur conserve néanmoins ses droits de propriété intellectuelle, dont son droit d'auteur, sur cette œuvre. Il est donc interdit de reproduire ou de publier en totalité ou en partie ce document sans l'autorisation de l'auteur.

Warning

The library of the Cégep de l'Abitibi-Témiscamingue and the Université du Québec en Abitibi-Témiscamingue obtained the permission of the author to use a copy of this document for non-profit purposes in order to put it in the open archives Depositum, which is free and accessible to all.

The author retains ownership of the copyright on this document. Neither the whole document, nor substantial extracts from it, may be printed or otherwise reproduced without the author's permission.

To My Family

REMERCIEMENTS

Firstly, I would like to thank my family for being with me since the first day of my life and for supporting me in every spare of my life.

I immensely express my gratitude to my director Professor Nahi Kandil, for giving me the opportunity to do research under LRTCS, for providing me the financial support during my study period. He provided me endless support as well as the assistance to complete my master's thesis; especially showed me and taught me the base of research, giving me the lesson about time management, professionalism.

I am deeply thankful to my co-director Professor Nadir Hakim for his continuous support and suggestions. He watched me in every step and guided me till the end. I am also grateful for giving me the valuable time and for supporting me in every difficulties.

Last, but not least, I would like to thank my colleagues in LRTCS, for helping me and to discussing with me about the problems and corresponding solutions regarding my research.

Thank you

Biki Barua

TABLE DES MATIÈRES

Chapitre 1	7
Introduction	7
1.1. Motivation in Wireless Sensor Network	7
1.1.1. History of wireless sensor network (WSN)	8
1.1.2. Comparison between traditional and wireless sensor network	10
1.2. Applications of Wireless Sensor Network	10
1.2.1. Wireless sensor network (WSN) in underground mine	11
1.3. Challenges and Constrains in Wireless Sensor Network	13
Chapitre 2	16
Ultra wide band localization	16
2.1. Definition of Ultra Wide Band System	16
2.2. Classification of Ultra Wide Band (UWB) System	18
2.2.1. Comparison of UWB technologies	18
2.2.2. Impluse radio (IR) Ultra wide band.....	19
2.2.3. Multi band (MB) Ultra wide band	23
2.3. Challenges of Ultra wide band system	25
2.4. Ultra wide band (UWB) in Localization	25
Chapitre 3	27
Localization techniques	27
3.1. Overview of Localization	27
3.2. Different Localization techniques	29
3.2.1. Receiving Signal Strength Indicator (RSSI)	29

3.2.2.	Angle of Arrival (AOA).....	30
3.2.3.	Time of Arrival (TOA)	30
3.3.	Why not GPS ?.....	33
3.4.	Evaluation of different localization techniques with UWB	34
<i>Chapitre 4</i>	<i>39</i>
<i>Our Approach, simulation and results</i>	<i>39</i>
4.1.	Overview of our localization structure	39
4.2.	Channel model	41
4.3.	Simulation results	44
4.3.1.	Localization via TOA	44
4.3.2.	Localization via TDOA and channel parameters effect	45
4.4.	Measurement Scenarios	49
4.4.1.	Indoor scenario	49
4.4.2.	Underground mine scenario	51
4.4.3.	Used sensors	54
4.5.	Measurement Results	57
4.5.1.	Indoor scenario	57
4.5.2.	Underground mine scenario	62
<i>Conclusion</i>	<i>65</i>
<i>Références</i>	<i>677</i>
<i>Appendix A</i>	<i>71</i>

LISTE DES FIGURES

FIGURE 1.1: MECHANISM OF WIRELESS SENSOR NETWORK	7
FIGURE 1.2: APPLICATIONS OF WIRELESS SENSOR NETWORK	11
FIGURE 2.1: LOW, CENTRAL AND HIGH FREQUENCIES OF AN UWB SYSTEM.....	17
FIGURE 2.2: IR UWB SIGNAL.....	21
FIGURE 2.3: SCHEMATIZATION OF THE GENERATION PROCESS FOR PPM-TH-UWB.....	22
FIGURE 2.4: SCHEMATIZATION OF THE GENERATION PROCESS FOR PAM-DS-UWB.....	22
FIGURE 2.5: PROPOSED MB-OFDM FREQUENCY BAND PLAN.....	25
FIGURE 3.1: CLASSIFICATION OF LOCALIZATION.....	28
FIGURE 3.2: ONE-WAY TOA.....	31
FIGURE 3.3: TWO-WAY TOA.....	32
FIGURE 3.4: TIME DIFFERENCE OF ARRIVAL ALGORITHM (TDOA).....	33
FIGURE 4.1: ANCHOR NODES POSITION PATTERNS.....	40
FIGURE 4.2: SALEH-VALENZUELA CHANNEL MODEL	41
FIGURE 4.3: POSITIONING ERROR FOR TOA.....	45
FIGURE 4.4: (A) AND (B) REPRESENTS THE EFFECT OF CLUSTER NUMBER CHANGES OVER MEAN EXCESS DELAY AND RMS DELAY SPREAD.....	407
FIGURE 4.5: (A) AND (B) REPRESENTS THE EFFECT OF RAY NUMBER CHANGES OVER MEAN EXCESS DELAY AND RMS DELAY SPREAD.....	48
FIGURE 4.6: MEASUREMENT SCENARIOS FOR NANOTRON.....	50
FIGURE 4.7: MEASUREMENT SCENARIOS FOR DECAWAVE.....	50
FIGURE 4.8: CITÉ DE L'OR MINE, VAL-D'OR.....	51
FIGURE 4.9: CITÉ DE L'OR MINE MAP.....	52
FIGURE 4.10: SETUP MEASUREMENT INSIDE MINE TUNNEL.....	53
FIGURE 4.11: MEASUREMENT SCENARIO FOR LOS.....	53
FIGURE 4.12: MEASUREMENT SCENARIO FOR NLOS.....	54
FIGURE 4.13: NANOTRON SENSOR.....	ERROR! BOOKMARK NOT DEFINED. 5
FIGURE 4.14: DECAWAVE SENSOR.....	56
FIGURE 4.15: MEASUREMENT USING NANOTRON FOR LOS.....	ERROR! BOOKMARK NOT DEFINED. 8
FIGURE 4.16: MEASUREMENT USING NANOTRON FOR NLOS.....	59
FIGURE 4.17: CHANNEL IMPULSE RESPONSE FOR LOS.....	60
FIGURE 4.18: CHANNEL IMPULSE RESPONSE FOR NLOS.....	61

FIGURE 4.19: MEASUREMENT AND SIMULATION USING DECAWAVE FOR LOS.	61
FIGURE 4.20: MEASUREMENT AND SIMULATION USING DECAWAVE FOR NLOS.	62
FIGURE 4.21: MEASUREMENT USING DECAWAVE FOR LOS (UNDERGROUND MINE).....	63
FIGURE 4.22 : MEASUREMENT USING DECAWAVE FOR NLOS (UNDERGROUND MINE).....	64

LISTE DES TABLEAUX

TABLEAU 1.1: DIFFERENCE BETWEEN TRADITIONAL AND WIRELESS SENSOR NETWORK	10
TABLEAU 2.1: DIFFERENCE BETWEEN IR AND MB UWB	19
TABLEAU 3.1: COMPARIOSN OF UWB SYSTEM	34
TABLEAU 4.1: IEEE UWB CHANNEL MODEL	42
TABLEAU 4.2: OPERATIONAL MODE.....	57

RÉSUMÉ

La sécurité et la communication posent des problèmes majeurs auxquels il faut remédier dans les environnements hostiles comme les mines souterraines. Pour une communication fiable ainsi que pour tracer la position exacte d'un objet dans les mines souterraines, différentes technologies ont été déployées. Parmi ces dernières, le réseau de capteurs sans fil est considéré comme un outil prometteur pour les applications basées sur la localisation, à savoir, la surveillance des lieux, le repérage des mobiles et la navigation. En fait, les réseaux de capteur sans-fil fournissent une couverture d'une vaste gamme d'équipements fiables, efficaces, tolérants aux défaillances et évolutives.

Cependant, les travaux de recherches précédents ont divisé la localisation en deux parties: les méthodes basées sur la portée et celles non-basées sur la portée. Où la première est précise et coûteuse tandis que la deuxième est présentée pour réduire la quantité d'énergie consommée du côté capteur dont les ressources sont limitées. Notre recherche se focalise sur la localisation basée sur la portée utilisant le réseau de capteurs sans fil dans les milieux internes et mines souterrains. Plusieurs techniques ont été proposées pour la localisation comme la réception de l'indicateur de force de signal (RSSI), le temps d'arrivée (TOA), la différence de temps d'arrivée (TDOA), l'angle d'arrivée (AOA). Bien que plusieurs travaux de recherches utilisant ces techniques aient été exécutés, l'approche de localisation à base de temps pour les environnements complexe comme la mine souterraine demeure limitée.

Cette thèse offre de nouvelles solutions pour combler l'écart entre la localisation à base de temps et le réseau de capteurs sans fil à haute précision, pour l'environnement minier souterrain. De plus, nous avons utilisé une technologie émergente, à savoir les communications ultra-large bande, pour booster la performance et l'exactitude. Notre travail de recherche est subdivisé en deux principales parties : une partie simulation et une partie pratique. Dans la première, nous avons utilisé MATLAB pour faire les différentes simulations. La deuxième partie consiste en plusieurs mesures pratiques

réalisées dans un environnement intérieur ainsi que dans une mine souterraine. Les résultats montrent une amélioration remarquable et une meilleure précision de la technique UWB à base de temps.

ABSTRACT

Safety and communication have always been a concerning issue in the harsh environments like underground mines. To make the communication reliable and to track the accurate position of the object in the underground mine, different technologies have been deployed. Among all the technologies, Wireless sensor networks (WSN) have been considered as promising tools for many location dependent applications such as area surveillance, search and rescue, mobile tracking and navigation, etc., where WSN provides a wide range of coverage in the terms of low cost, reliable, efficient, fault tolerant and scalable facilities.

However, previous research divided the localization into two parts: range base and range free, where range base method is accurate and costly and range free technique is featured to reduce the overhead at the resource constrained sensor node side. Our research is focusing on range base localization using wireless sensor network for both indoor and underground mine environments respectively. There are several techniques has been proposed for localization such as receiving signal strength indicator (RSSI), time of arrival (TOA), time difference of arrival (TDOA), angle of arrival (AOA). Even though, a large sum of researches has been performed using those techniques, the time base localization approach for the harsh environments like underground mine is still limited.

This thesis offers novel solutions to bridge the gap between time base localization and WSN with high accuracy for underground mine. Besides, we have used emerging technology like ultra-wide band (UWB) to boost the performance and accuracy. To achieve the research aim, we have design our research outline into two categories: simulation and practical measurement. Using MATLAB simulation tools extensive simulation has been performed. Afterwards, a large number of practical measurements

also been performed in indoor and underground mine environment. The results show remarkable improvement and accuracy of the time base UWB scheme.

GLOSSAIRE

WSN	Wireless sensor network
LOS	Line of sight
NLOS	Non line of sight
TOA	Time of arrival
TDOA	Time difference of arrival
AOA	Angle of arrival
RMSE	Root mean square error
PM	Path magnitude
PSD	Power spectral density
MB	Multi band
IR	Impulse response
PPM	Pulse position modulation
PAM	Pulse amplitude modulation
TH	Time hopping
DS	Direct sequence
WPAN	Wireless Personal Area Networks
OFDM	Orthogonal frequency-division multiplexing
ADC	Analog to Digital converter
GPS	Global positioning system
GHz	Giga hertz

LISTE DES VARIABLES

f_c	Central frequency
f_L	Lower frequency
f_H	Higher frequency
B_{frac}	Fractional bandwidth
nsec	Nano second
R_b	Binary sequence generation rate
N_s	Number of repetition code
T_s	Frame time
$\delta(t)$	Dirac Pulse
c	Binary code
N_s	Number of repetition code
T_s	Frame time
$\delta(t)$	Dirac Pulse
c	Binary code
η	Constant attenuation
P	Transmission power
C	Speed of light
τ	Delay
D	Distance
λ	pulse arrival rate
Λ	Cluster arrival rate
Γ	Power delay factor for pulse
γ	Power delay factor for pulse in cluster
σ_ξ	standard deviation of the fluctuation of the channel coefficient for the clusters.
σ_ζ	The standard deviation of the fluctuation of the channel coefficient for pulse within each cluster.
σ_g	The standard deviation of the channel amplitude gains.

CHAPITRE 1

INTRODUCTION

1.1. Motivation in Wireless Sensor Network

In the new era of technology, wireless sensor network (WSN) strongly holds a vital position in the research community because of its natural involvement, characterization and potentiality in application. Furthermore, the researchers also give a big emphasize on WSN in order to build a strong, efficient and flexible network. Moreover, the advancement in nanotechnology, such as micro electromechanical systems (MEMS), in wireless communications increases the capability of sensing, data processing and communication. That realization and adaptation put the wireless sensor network (WSN) in high priority. In wireless sensor network (WSN) a larger number of autonomous sensors is distributed in the environment to monitor the physical or environmental conditions, such as temperature, sound, pressure, etc. and to cooperatively pass their data through the network to a main location.

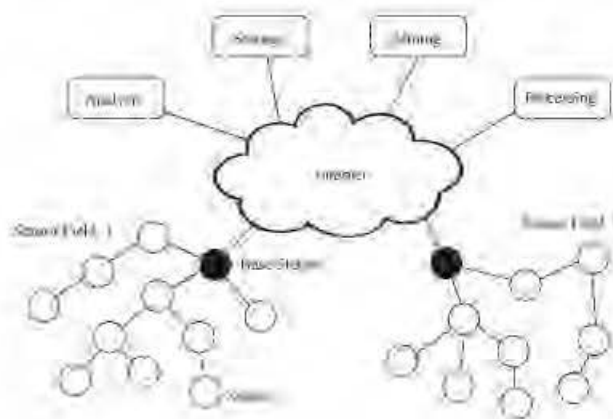


Figure 1.1: Mechanism of Wireless Sensor Network [3].

Most importantly in wireless sensor network, many sensors are connected to controllers as well as to the processing stations directly. That's increase the adaptability and the deployment of thousands sensors for many network applications in remote areas. That's why a wireless sensor not only work as a sensing component, but also work as an on-board processing, communication and storage capabilities. Nevertheless, the capabilities of the nodes in the sensor network vary widely. For instance, simple sensor nodes are just used to monitor the physical phenomenon, while more complex sensors are not only used to monitor. An extensive example for complex sensor is PING, SRF 04/05, ultrasonic devices measuring the distance to the object using sonar technology. However, an overall application and functionality of the wireless sensor network is given below:

However, an overall application and functionality of the wireless sensor network is given below:

- This system can generate pre-alarms and can define the different alarm conditions based on the emergency.
- It provides the efficient power technique to increase the operational time [4].
- WSN provides different node architecture that follows up the application on the efficient mode.

1.1.1 History of Wireless Sensor Network (WSN) [2]:

Discerning about WSN or sensor network was started in early 1950, with the development of the first wireless network that bore any real resemblance to a modern WSN which was the Sound Surveillance System (SOSUS), developed by the United States Military in the 1950s to detect and track Soviet submarines. After that, in 1978, the agency of United States department of defense, called Defense Advanced Research Projects Agency (DARPA), organized a workshop named the Distributed Sensor Nets

(DSN), where the aim was to focus on sensor network research challenges such as networking technologies, signal processing techniques, and distributed algorithms. So, couple of academia's such as Carnegie Mellon University and the Massachusetts Institute of Technology Lincoln Labs, were linked and grouped to perform the research under DSN and through that WSN technology found a homeland for WSN research. After that, low Power Wireless Integrated Micro sensor (LWIM) was the first outcome of the WINS project and produced in 1996, while the smart sensing system was based on a Complementary metal-oxide-semiconductor (CMOS) chip, integrating multiple sensors, interface circuits, digital signal processing circuit's wireless radio, and microcontroller onto a single chip [3]. But, in 2001 University of California at Los Angeles with the collaboration of Rockwell Science Center proposed the concept of Wireless Integrated Network Sensors or WINS. However, afterwards several research projects have been run, such as The PicoRadio project by the Berkeley Wireless Research Center (BWRC) in 2002 focusing on low-power sensor devices, μ AMPS (micro-Adaptive Multi-domain Power-aware Sensors) project by MIT [3] in 2005 focusing on low-power hardware and software components for sensor nodes, including the use of microcontrollers capable of dynamic voltage scaling and techniques to restructure data processing algorithms to reduce power requirements at the software level. And the outcomes of those projects are remarkable and playing a vital role in WSN by reducing the complexity of the sensor network, making high efficient along with improved sensors. Since, after that wireless sensor network (WSN) reaches to the remarkable advancement throughout in different applications such as for localization in indoor and outdoor environment, underwater tracking, sensing the different physical parameters etc.

1.1.2 Comparison Between Traditional and Wireless Sensor Network:

Table 1.1 shows some key differences between traditional network and wireless sensor network. Where traditional sensor network is a general-purpose application that's projected to perform specific aim within normal condition.

Tableau 1.1: Difference between traditional & wireless sensor network

Traditional Network	Wireless sensor network
General Purpose design and serving many application	Single-purpose design; serving one specific Application
Obtaining global network knowledge is typically feasible and centralized management is possible	Most decisions are localized without the support of a central manager
Component failure is addressed through maintenance and repair	Component failure is expected and addressed in the design of the network
Maintenance and repair are common and networks are typically easy to access	Physical access to sensor nodes is often difficult or even impossible
Devices and networks operate in controlled and mild environments	Sensor networks often operate in environments with harsh conditions
Networks are designed and engineered according to plans	Deployment, network structure, and resource use are often ad hoc (without planning)
Typical primary design concerns are network performance and latencies; energy is not a primary concern	Energy is the main constraint in the design of all node and network components

1.2. *Applications of Wireless Sensor Network*

Wireless sensor network (WSN) have a wide range of involvement in different application and inspiringly increase the involvement in new different application. The

diversity of applications in the following categories is remarkable – environmental monitoring, target tracking, pipeline (water, oil, gas) monitoring, structural health monitoring, precision agriculture, health care, supply chain management, active volcano monitoring, transportation, human activity monitoring, and underground mining, to name a few. However, this section discusses in details application of wireless sensor network (WSN) in underground mine.

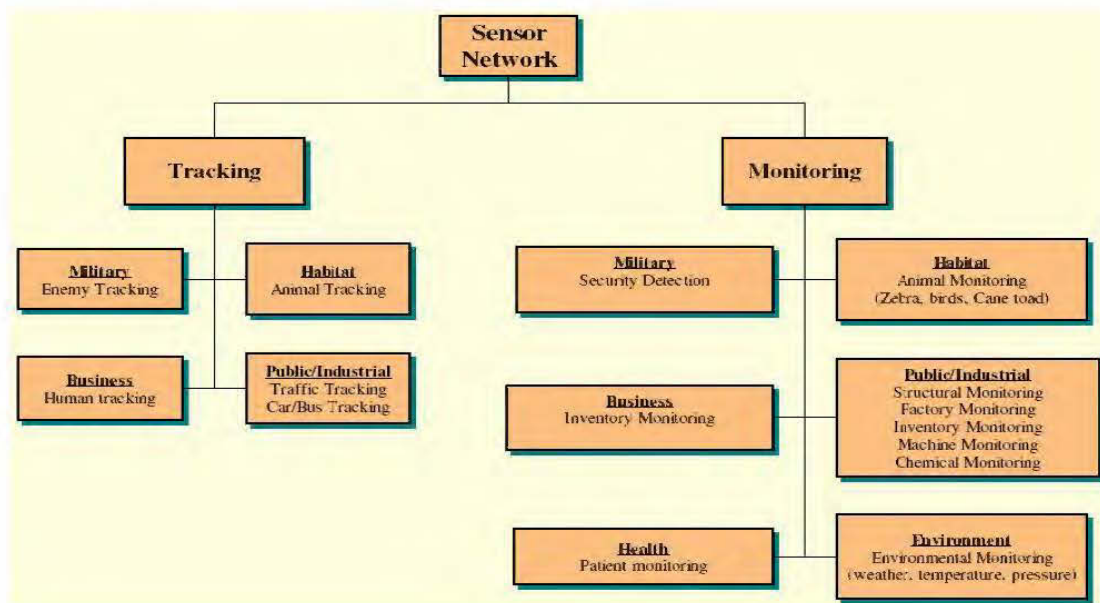


Figure 2.2: Applications of Wireless Sensor Network.

1.2.1 Wireless Sensor Network (WSN) in Underground Mine:

Underground mine is one of the most vital application field of wireless sensor network (WSN). Underground mines are considered as the most dangerous application field, where WSN perform different function such as: tracking, sensing, computing, distance measurement etc. In order to make people understand the risks associated with underground mines, we present an example, in which we also present the involvement of WSN in example.

The incident happened at Crandall Canyon mine, Utah, USA in 3 August 2007 [5]. At that time, six miners were trapped inside the coal mine. Even though their accurate location was not known, experts estimated that the men were trapped 457m below ground, 5.5 km away from the mine's entrance. There were different opinions about the exact cause of the accident. The owners of the mine claimed that a natural earthquake was the cause. However, Seismologists at the University of Utah observed that seismic waves of 3.9 magnitude had been recorded on the same day in the area of the mine, leading scientists to suspect that mine operations were the cause of the seismic spikes. However, afterwards an immediate rescue attempt was undertaken. That's included the drilling of 6.4 cm and 26 cm holes into the mine cavity, where an omnidirectional microphone and a video camera were lowered, and an air sample was taken. The air sample indicated the presence of sufficient oxygen (20%), a small concentration of carbon dioxide, and no trace of methane. The microphone detected no sound and the video camera revealed some equipment, but not the six missing miners [3]. But later on due to the lack of proper management and technology, six miners were found dead later.

However, from this example of fatal accident we can describe the involvement and application of WSN network.

1. WSN can collect different data's such as temperature, existence of different gases with existence concentration, detection of ground plate movement with proper value, by deploying different types of sensors. These data's used to analyze the physical conditions and able to predict the situation, that might be a great initiative to overpass the unwanted accident.

2. By installing multi-functional sensors in remote locations whole areas can be bring over under the observation using WSN. That reduces human risk and ignores the fatal accident.

3. Introducing a high-level of vision for localization technique in underground mine using WSN can provide the strong monitoring and precision about the position of miner and object.

1.3. Challenges and Constrains in Wireless Sensor Network

In the practical application of wireless sensor network there are subject to a variety of unique challenges and constraints. Where to determine the object position is the major aim in sensor application and makes the network's energy efficient. Therefore, localization is the task of determining the physical coordinates of a sensor node [4]. Localization collects information about longitude, latitude and attitude of the sensor network. While tracking is a way to identify the moving object or the miner with the context of the anchor node (anchor node is also called reference node & it's position along with other data is always known) that are already set up by the localization technique. However, several challenges can limit the efficiency of the localization such as physical layer measurement errors, computation constraints, lack of GPS data, low-end sensor nodes, and architecture. Moreover, WSN applications pose different requirements for localization protocols in terms of scalability, robustness, and accuracy. In essence, there are some other factors; those put the WSN in big challenge:

a. **Fault Tolerance:** Sensor network should remain functional even if any node fails while the network is operational. The network should be able to adapt by changing its connectivity in the case any fault happens. In this situation, well- efficient routing algorithm is applied to change the overall configuration of the network [6].

b. **Energy:** Energy is one of the main aspects, not only for localization but also in the whole WSN. Energy is consumed in data collection, data processing, and data communication. It also enable the continuous operations between the base nodes to the mobile nodes. Batteries is the source to provide power or energy, besides it's needed to be changed or recharged after they have been consumed. Sometimes it becomes difficult to recharge or change the batteries because of demographic conditions. The

most crucial research challenge for the WSN researchers is to design, develop and implement energy efficient hardware and software protocols for WSNs.

c. Self-Management: In wireless sensor networks, once nodes are deployed, they should be able to work without any human intervention. They should be able to manage the independent operation, approachment localization, network configuration, adaptation, maintenance, and self-reparation.

d. Calibration: Sensor Calibration is the process of adjusting the raw sensor readings obtained from the sensors into corrected values by comparing them with some standard values. In the localization, to find out the perfect position of the unknown node, the value of calibration is much important. Except for this, it is hard to improvise the localization algorithm.

e. Secure Localization: Often, the utility of a sensor network will rely on its ability to accurately and automatically locate each sensor in the network. A sensor network is designed to locate faults. For that, accurate location information is needed in order to pinpoint the location of a fault [7]. Unfortunately, an attacker can easily manipulate non-secured location information by reporting false signal strengths, replaying signals, etc.

However, in the process of WSNs localization, a common problem is how to mitigate the non-line-of-sight (NLOS) error that inevitably occurs in many cases. Therefore, in order to prove the localization accuracy, some related approaches are proposed to reduce this error. Although, there is a lot of progress occurring in the field of WSN, there are still some challenging problems such as strong Sturdiness and real-time performance that need attention. In our research, we will go through these challenges and we will try to improve the localization technique, so that we can obtain a good performance.

CHAPITRE 2

ULTRA WIDE BAND LOCALIZATION

2.1. Definition of Ultra Wide Band System

Ultra-wideband (UWB), the most fame and efficient as well as rapid breeding technology for communication. The research establishment about UWB has been started since early 1990s, resulting the pioneering work of Win and Scholtz at University of Southern California (USC). the Federal Communications Commission (FCC) allows unlicensed operation of UWB transmission subject to certain restrictions in the emission mask of the power spectral density. And the allowed the frequency band for UWB in between 3.1 and 10.6 GHz with a power spectral density of -41.3 dBm/MHz.

The minimum bandwidth of the Ultra-wideband (UWB) signals are defined to have at least 500 MHz and/or a relative bandwidth of more than 20% [8]. However, the f_c should be larger than 2.5 GHz, or have a fractional bandwidth (B_{frac}) that is larger than 0.2 for systems with f_c lower than 2.5 GHz. Where, f_c is the frequency in maximum power density and the frequencies f_H and f_L determine the location where the power spectral density is 10 dB below the f_c . So, B_{frac} (fractional bandwidth) is defined as [9]:

$$B_{frac} = \frac{B}{f_c} \quad (2.1)$$

Where, B is indicating the Bandwidth of the system. Besides, for higher and lower frequency:

$$f_c = \frac{f_H + f_L}{2} \quad (2.2)$$

$$B_{frac} = \frac{2(f_H - f_L)}{f_H + f_L} \quad (2.3)$$

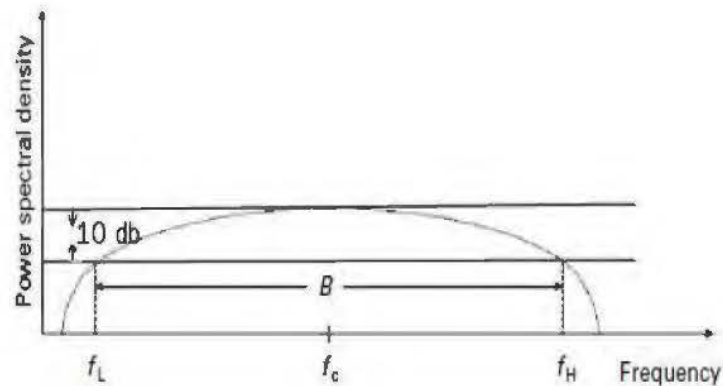


Figure 2.1: Low, central and high frequencies of an UWB system.

However, there are some unique advantages in UWB signal. Such as:

- a) The most vital characteristic of UWB is the large bandwidth in comparison with prevalent narrow-band systems.
- b) Small-scale fading, good resolution for ranging and geolocation.
- c) Resistance to narrow-band interference.
- d) These signals can be used for transmission of extremely high-speed data or low rate data with a large spreading factor.
- e) Less interference with other communication signal.
- f) Due inverse relation between time and frequency, the time resolution of UWB signals is high and makes UWB a good candidate for positioning systems.
- g) UWB is permitted to occupy lower carrier frequency that allows the UWB signal to pass through obstacles.

h) UWB signals can be transmitted in base band. Therefore, there is no need for Intermediate Frequency (IF) multipliers in transceivers. This property can lead to less expensive to aim project.

i) The high time resolution and short wavelength of UWB signals strengthen it against multipath interference and fading.

2.2. Classification of Ultra Wide Band (UWB) System

Ultra wide-band (UWB) technology are divided into two technologies. Those are:

- Impulse radio (IR) UWB
- Multiband (MB) UWB

Impulse radio (IR) UWB conventionally been emitted by radiating pulses that are very short in time, typically a few nanoseconds. This technique is basically used in military radar application, tracking and identification of object [11]. On the other hand, multiband UWB (MB) uses frequency hopping method with Orthogonal Frequency Division Multiplexing (OFDM). In our work we have used IR UWB as a communication tool for positioning and ranging between sensors. The reason is that IR UWB provides a better functionality in the physical layer by transmitting the maximum effect of available spectrum over MB UWB [12]. Moreover, IR UWB operates at a very large bandwidth at low power. In addition, it creates short pulses (shorter than 1 nanosecond), as well as its resistance to multipath propagation, allowing the system to achieve highly accurate measurements in ranging especially in the indoor environment [12].

2.2.1 Comparison of UWB Technologies

However, a comparison in between IR and MB UWB technologies in the term of interference with other systems, performance, sturdiness to multipath, system's

complexity and achievable range-data rate performance for the WPAN applications, is given below:

Tableau 2.1: Difference between IR and MB UWB

Specificati on	IR UWB	MB UWB
Number of sub-band	2 (3.1-4.58 GHz) (6.2-9.7GHz)	3 mandatory & up to 14
Bandwidth of sub-band	1.75 GHz for lower band 3.5 GHz for higher band	528 MHz
Number of sub carrier	No sub carrier (Baseband signal)	122
Spreading factor	1 – 24	1,2
Data rates	28,55,110,220,500,660,1000, 1320 Mbps (lower band)	55,80,110,160,200,320, 480 Mbps
Modulation	BPM, MBOK	QPSK
Multiple excess	Based on PM codes	Based of time frequency code

2.2.2 Impulse Radio (IR) Ultra-wide Band

In IR UWB, the UWB signal is used to emit at a very high data rate, where the emitting signal is generated by generating pulses in a very short time, almost in sub-nanosecond [13]. Basically, the impulse radio UWB is a carrier-less transmission and,

due to narrow pulses, the spectrum of the signal reaches several GHz of bandwidth. Furthermore, this technology has a low transmit power and because the narrowness of the transmitted pulses has a fine time resolution the implementation of this technique is very simple, as no mixer is required which means low cost transmitters and receivers.

In essence, IR UWB technique can be divided into two different methods. Those are:

- Time Hopping (TH) UWB
- Direct Sequence (DS) UWB

These IR methods DS-UWB and TH-UWB are differentiated by multiple access techniques that spread signals over a very wide bandwidth. Because of spreading signals over a very large bandwidth, the IR technique can combat interferences from other users or sources [14]. It should be mentioned that Direct Sequence Spread Spectrum (DSSS) and Time Hopping Spread Spectrum (THSS) might be considered similar to DS-UWB and TH-UWB, respectively. However, there are some differences between the spread spectrum and IR-UWB systems. Both systems take advantage of the expanded bandwidth. However, different methods are used to obtain such large bandwidth. In the conventional spread-spectrum techniques, the signals are continuous-wave sinusoids that are modulated with a fixed carrier frequency, while in the IR-UWB (i.e., DS-UWB and TH-UWB), signals basically are baseband and the narrow UWB pulses are directly generated having an extremely wide bandwidth. Another difference is the bandwidth. For the UWB signals the bandwidth has to be higher than 500MHz, while for the spread spectrum techniques bandwidths are much smaller (usually in the order of several MHz) [14].

Information and data symbols at IR UWB are modulated by two different methods, where Pulse amplitude modulation (PAM) and Pulse position modulation (PPM) are most commonly accepted modulation schemes. Based on the data rate and

characteristics, both TH UWB and DS UWB can choose either PAM or PPM modulation technique.

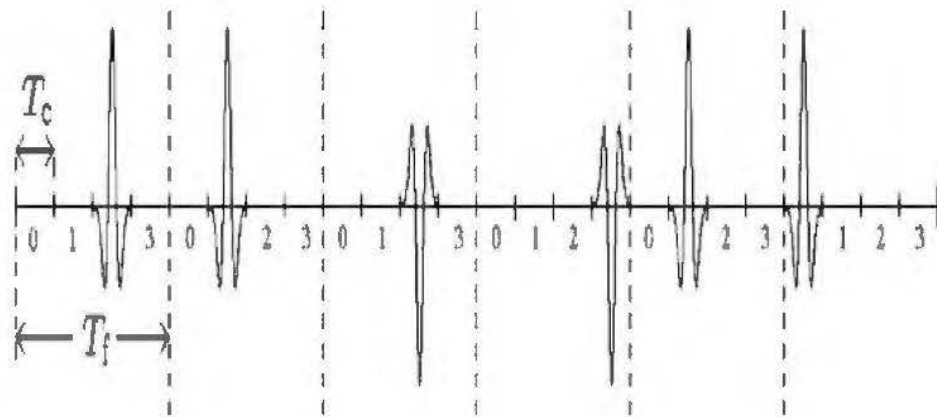


Figure 2.2: IR UWB Signal [9].

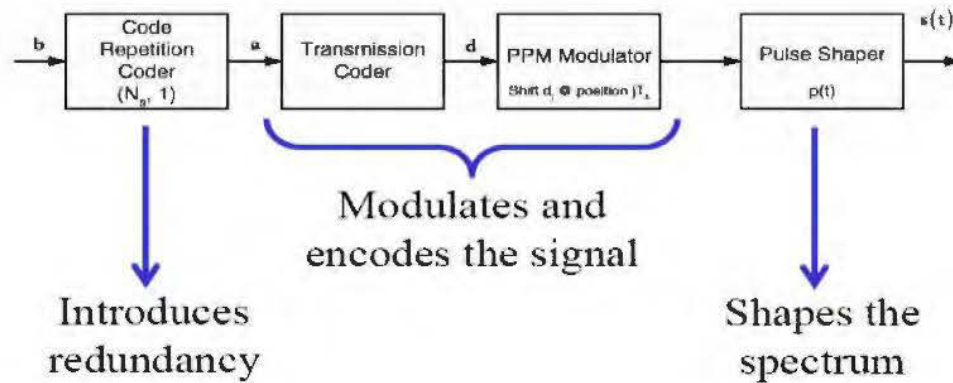


Figure 2.3: Schematization of the generation process for PPM-TH-UWB [11].

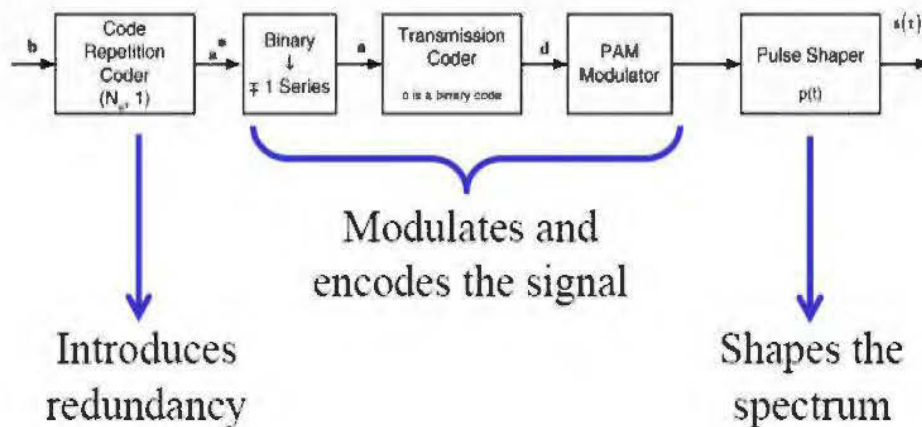


Figure 2.4: Schematization of the generation process for PAM-DS-UWB [11].

Figure 2.3 shows the TH-UWB with PPM modulator [11]. The process starts with the repetition coder. A binary sequence b is generated at a rate of $R_b = 1/T_b$ bits/s and the repetition coder repeats each bit N_s times and generates a binary sequence at a rate of $R_{cb} = N_s/T_b = 1/T_s$ bits/s, where T_s is the frame time. Termination is introduced in this way and the system is seen as a $(N_s, 1)$ repetition coder. In the second phase, transmission coder generates a new sequence d by applying an integer-valued code c to the previously generated sequence a . PPM modulator represents the third phase. It

receives the sequence d and produce a series of the Dirac pulses ($\delta(t)$) at the rate of $R_p = N_s/T_b = 1/T_s$. At the end, the shape of generated signal is shaped by pulse shaper.

On the other hand, figure 2.4 shows the DS-UWB generation process with PAM modulator. Likewise, before the process starts with the repetition coder. A binary sequence b is generated at a rate of $R_b = 1/T_b$ bits/s. In the next stage, binary series change the sequence of a to the a^* which is composed of binary antipodal symbol (± 1). In the third phase transmission coder applies a binary code c consisting of (± 1) and with period N_p to the sequence a . So, a new sequence $d = a * c$ is generated. Then as a sequences d enters is PAM-modulator where a sequence of Dirac pulses Dirac pulses ($\delta(t)$) positioned at jT_s is generated at a rate of $R_p = N_s/T_b = 1/T_s$. At the end, the pulse shaper conduct its shaping operation.

2.2.3 Multi Band (MB) Ultra-wide Band

Multi-Band UWB is a second fundamental method of UWB technology where OFDM method has been used and functionally altered from previous IR UWB. Multi-Band OFDM combines the OFDM technique with the multi-band approach. The spectrum is divided into several sub-bands with a -10 dB bandwidth of at least 500 MHz.

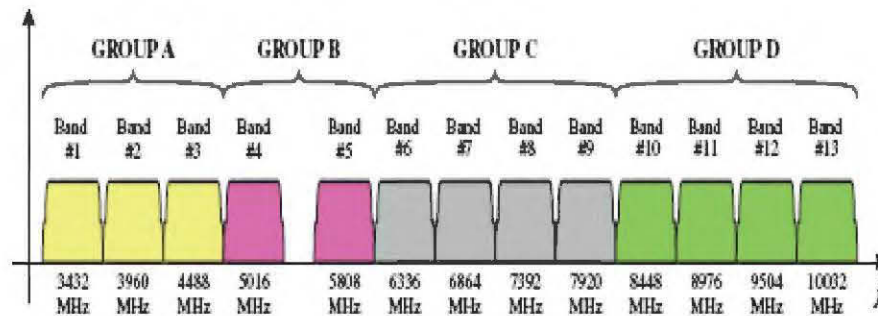


Figure 2.5: Proposed MB-OFDM frequency band plan.

The information is then interleaved across sub-bands and later transmitted through multi-carrier (OFDM) technique [13]. One of the proposals for the physical layer standard of future high speed Wireless Personal Area Networks (WPANs) uses the MB-OFDM technique. In this MB-OFDM WPANs proposal, the spectrum between 3.1 and 10.6 GHz is divided into 14 bands with 528MHz bandwidth that may be added or dropped depending upon the interference from, or to, other systems. In figure 2.5, a possible band plan is presented, where only 13 bands are used to avoid interference between UWB and the existing IEEE 802.11a signals. The three lower bands are used for standard operation, which is mandatory, and the rest of the bands are allocated for optional use or future expansions. MB-OFDM technology promises to deliver data rates of about 110 Mbps at a distance of 10 m [15]. For the UWB wireless sensor applications, data rates are low, but the (hoping) coverage might be much larger than 10 m. MB-OFDM may require higher power levels when compared to the IR technology.

2.3. Challenges of Ultra Wide Band System [10]

Besides the advantages, there are some disadvantages that put the UWB technology in a challenging position.

a) Channel Estimation: To design an efficient receiver in wireless communication, channel estimation plays a complete vital role. As it is impossible to estimate every signal channel in the communication environment, so an example pre-define sequence is used setup in receiver in order to measure the different channel parameter's such as delay, power, etc. To design it, in every UWB receiver a pre-defined signal template is formatted and correlated. Therefore, when the receiver receives the real signal that is wide band and low powered, the UWB pulses undergo severe pulse distortion.

b) Time Synchronization: Time synchronization is considered a major challenge for UWB communications systems. Along with other communication systems, the time synchronization must be done in UWB transmitter/receiver pairs. However, sampling and synchronizing nanosecond pulses place a major limitation on the design of UWB systems. In order to sample these narrow pulses, very fast (on the order of gigahertz) analog-to-digital converters (ADCs) are needed. Moreover, the strict power limitations and short pulse duration make the performance of UWB systems highly sensitive to timing errors.

c) Pulse Shape Distortion: The transmission characteristics of narrow band signal are different than UWB signal. Basically a narrowband signal remains sinusoidal throughout the transmission channel, where the low powered UWB signal is significantly distorted. Moreover, in narrowband signal, the frequency changes bring out minimum changes in the receiving power, where for UWB signal it is totally different. Due to the wide range of frequencies that is covered by the UWB spectrum, the received power drastically changes and thus distorts the pulse shape.

2.4. Ultra Wide Band (UWB) in Localization

Being a promising technology at present, the involvement of UWB is referred to as a base-band, impulse, and carrier-free technology. However, most three well known application areas of UWB is given below:

- a. Communication and sensors
- b. Localization and tracking
- c. Radar

As our focus is on localization, in this section, we will only discuss about the application of UWB in localization.

Some key features of UWB such as high data rate, big bandwidth and extremely short pulse properties make the UWB a perfect application for localization [42]. For instance, higher data rate of property makes a good solution of the data transmission in nearby field for localization. Besides, the high bandwidth and extremely short pulses waveforms help in reducing the effect of multipath interference and facilitate determination of time base localization for burst transmission between the transmitter and corresponding receiver [43]. Low frequency properties of the UWB pulse allows the signal to pass through wall and make an accurate measurement. That's why at present situation UWB technology is considered as a one of most promising technology for localization.

However, even for complex situations like NLOS, UWB has advantages over other technologies. For example, UWB technology, unlike the other technology such as infra-red and ultrasound sensor, does not require a line-of-sight and is not affected by the existence of other communication devices or external noise [44]. This is also because of high bandwidth and signal modulation technique of UWB technology.

CHAPITRE 3

LOCALIZATION TECHNIQUES

3.1. Overview of Localization

Sensors monitor phenomena in the physical world plus the spatial relationships between sensors and the objects of the physical world are an essential component of the sensor information. Without knowing the position of a sensor node, the information conveys only the little part of the operation and information [31]. Therefore, localization is the task that is used to determine the physical position of an unknown sensor node. Even though, the Global Positioning System (GPS) is undoubtedly the most well-known location-sensing system, it is not accessible in all environments (e.g., indoors or under dense foliage) and may incur unacceptable resource costs for resource-constrained wireless sensor networks (WSNs).

In order to determine the position, localization uses different types of ranging and positioning technique. Ranging process is defined as computing the distance from which the target that needs to be localized (unknown node) to the reference node (a node which position is known). A reference node establishes a peer to peer communication to obtain ranging information regarding an unknown node in the sensor network. On the other hand, positioning is the process of computing the position of an unknown node with respect to the position of the reference node. However, in order to design a perfect localization technique for wireless sensor network, two main challenges should be taken into consideration: the accuracy and the efficiency of the technique [32].

Global positioning system (GPS) method has been widely used in localization, but it is costly in terms of power consumption, cost and physical aspects, as well as its

poor efficiency in the indoor and harsh environments. In order to overcome these issues and limitations in indoor and harsh environments, several localization methods have been proposed. These methods are divided into range base and range free methods [33] (c.f fig 3.1).

Range based localization methods, used where high accuracy is required, are based on distance and/or angle measurements between unknown and reference nodes. These measurements are used to estimate the unknown nodes' position. Several range based localization methods have been proposed in the literature such as the received signal strength indicator (RSSI), time of arrival (TOA), time difference of arrival (TDOA) and angle of arrival (AOA) [34] [35]. However, range free localization algorithms, used where accuracy is not so important, do not require distance or angle measurements between nodes. They are based on the connectivity between nodes in WSN. Common range free localization methods are hop count base localization (DV-Hop algorithm) and Pattern matching base localization [21]. However, in this chapter we will discuss about different range base localization techniques.

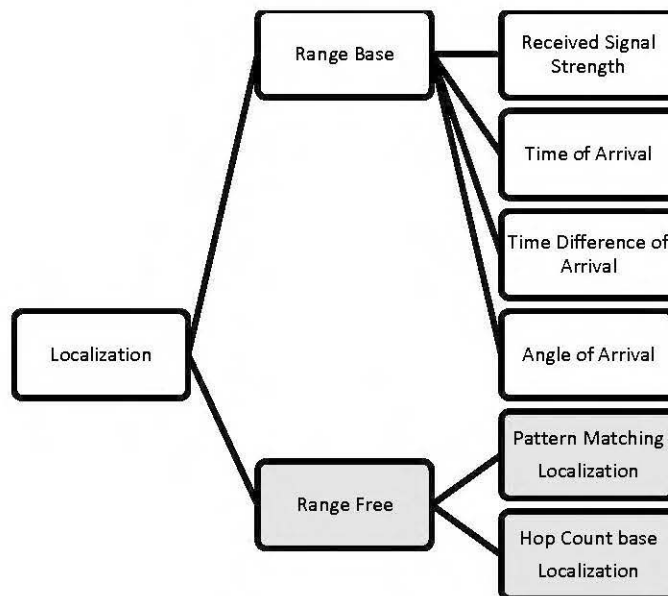


Figure 3.1: Classification of localization.

3.2. Different Localization techniques

3.2.1 Receiving Signal Strength Indicator (RSSI):

Among all the techniques in localization, RSSI is the most renowned one where the received signal strength is used to determine the distance, while signal strength determined by measuring the amplitude of the incoming radio signal [22]. Since each sensor node is equipped with a radio and is in most cases able to report the received signal strength of an incoming packet, this technique has minimal hardware requirements. In essence, to measure the distance following information are usually used:

- Receiving signal Power
- familiarity of the initial or transmitted power
- the path-loss model.

The received signal strength from sensor node i at node j at time t is represented by $P_R^{ij}(t)$, which is expressed as [23]:

$$P_R^{ij}(t) = P_T^i - 10\eta \log(d_{ij}) + X_{ij}(t) \quad (3.1)$$

Where $X_{ij}(t)$ is the uncertain factor due to shadowing and multipath effects, η is the constant attenuation and P_T^i is a constant due to the transmitted power and the antenna's gains of the sensor nodes.

There are some disadvantages that put the RSSI in front of big challenges. Like the effects of shadowing and multi-path as modeled by the term $X_{ij}(t)$ in equation (3.1) may be severe and require multiple ranging measurements. Moreover, in cases where there is no line of sight between a beacon and a node, the received signal strength measurements results in a significant error in distance measurements. Besides, the other major challenge with the RSSI-based distance measurements is the difficulty of estimating the parameters for the channel model. While the transmitted power may be

fixed for a localization application for each beacon node, the parameters associated with antenna's gains may differ from node to node. Moreover, the attenuation constant, η , varies with the environment. Hence, pre-deployment calibration may be required to estimate these parameters for localization algorithms.

3.2.2 Angle of Arrival (AOA):

Angle of arrival (AOA) technique is used in localization to determine the direction of signal propagation from the target node to the reference nodes. This is typically done by using an array of antennas or microphones. This technique provides high accuracy but also depends on the measurement's accuracy. Besides, AOA estimation algorithms are very sensitive to many factors, which may cause errors in their estimation of target position. In addition, the setup of the antenna array is quite complex and highly sensitive, where a small mistake brings out large disparity in the direction measurement. Moreover, the cost of hardware is very high in AOA technique [28]. So, the AOA technique can be used with other techniques to increase its accuracy.

In addition, AOA method is not well suited for UWB positioning. Use of antenna arrays is impossible when small and cheap sensors are of interest. The increased system costs introduced by the arrays directly contradicts the main advantage of UWB radio, which allows low-cost transmitters due to a large bandwidth. The large bandwidth of UWB signals creates additional problems regarding angle estimation. A large bandwidth implies a large number of possible paths from reference nodes to a target node. This leads to significant challenges in angle estimation due to multipath and scattering from objects in the environment [24].

3.2.3 *Time of arrival*

The time of arrival (TOA) technique rely on accurate measurements of transmitting and receiving time of signals between two nodes [32]. These measurements are used to estimate the distance based on the propagation time. Since

timing information is used for distance measurements, synchronization is essential for these techniques. Based on the measurement type, two types of TOA measurements can be performed [35]:

3.2.3.1 One way TOA:

In the one-way TOA technique, the projected delay for one-way propagation between sender and receiver is being measure to calculate the delay, where the propagation delay is counted by the difference between sending time and receiving time. Imagine that at time t_1 , node A transmits a packet to receiving node B that contains the time stamp t_1 . Node B receives the packet at time t_2 . Under ideal conditions, when node clocks are perfectly synchronized with the propagation delay τ_F is calculated by

$$distance_{AB} = (t_2 - t_1) * C \quad (3.2)$$

Where C is the velocity of light.

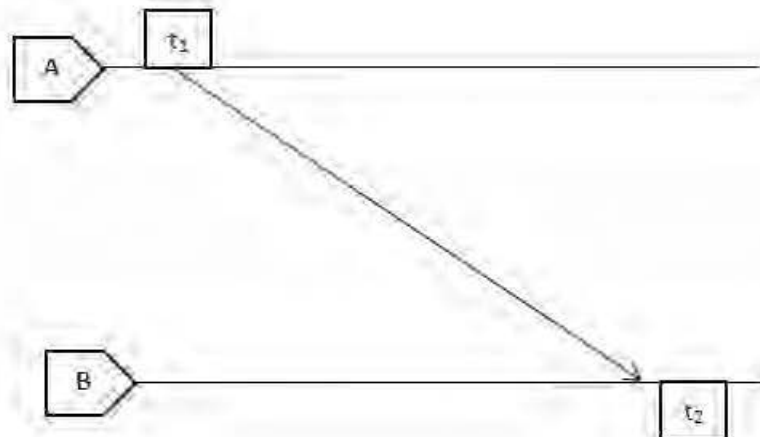


Figure 3.2: One way TOA

3.2.3.2 Two way TOA

In two-way ranging, the system estimates the signal round-trip time (RTT) without a common time reference. Node A transmits a packet to node B, which replies by transmitting an acknowledgment packet to A after a response delay t_d [35]. The RTT (round trip time) at A is determined by $\tau_{RTT} = 2T_f + t_d$ from which the distance can be estimated assuming t_d is known.

$$distance_{AB} = \frac{(t_4 - t_1) - (t_3 - t_2)}{2} * C \quad (3.3)$$

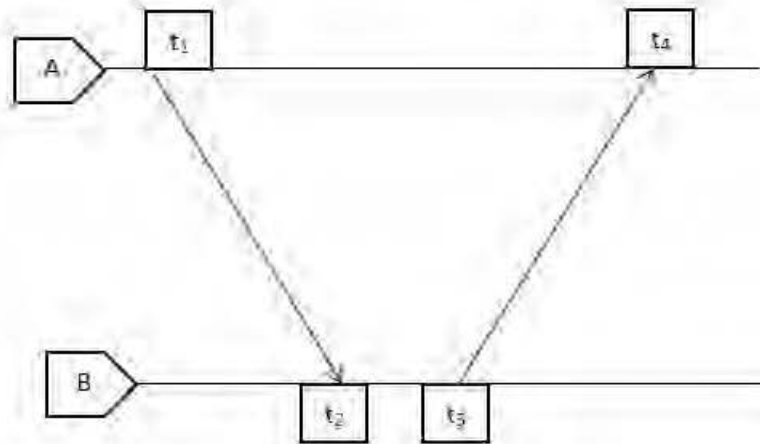


Figure 3.3: Two way TOA.

3.2.3.3 Time difference of arrival (TDOA)

Time difference of arrival (TDOA) algorithm is a range based distance-measuring technique where the delay between the receiving times of two received signals is used to estimate the distance between the nodes. The mathematical expression for calculating distance is given by:

$$D = \tau * C \quad (3.4)$$

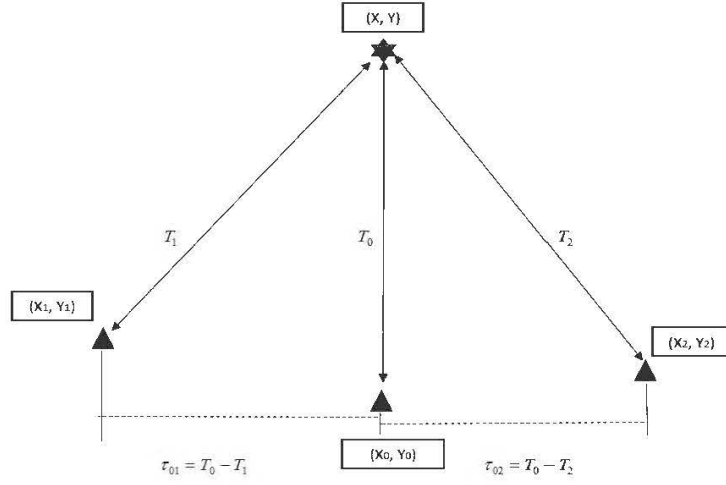


Figure 3.4: Time Difference of Arrival Algorithm (TDOA).

$$D_0 - D_1 = C * \tau_{01} = \sqrt{(x - x_0)^2 + (y - y_0)^2} - \sqrt{(x - x_1)^2 + (y - y_1)^2} \quad (3.5)$$

$$D_0 - D_2 = C * \tau_{02} = \sqrt{(x - x_0)^2 + (y - y_0)^2} - \sqrt{(x - x_2)^2 + (y - y_2)^2} \quad (3.6)$$

Where in equation (3.4) D is the measured distance, C is the velocity of light, and τ is the time delay. In equation (3.5) and (3.5), (x, y) represent the position of an unknown node as well as (x, y) represent the position of an unknown node as well as (x_0, y_0) , (x_1, y_1) and (x_2, y_2) which represent the position of the anchor node. Even though, both TDOA and TOA are time base techniques. Contrary to TOA algorithm, TDOA does not require the synchronization between the given node and reference or anchor.

3.3 Why not GPS?

GPS, a wide known global positioning system, where satellite communication system is used to track the object. In addition, this system is employed for localization

and tracking is different embedded system such as cell phone, navigation system and radar. Even though, GPS provides accurate information about localization and tracking, it is not perfectly fit for some specific environment. Firstly, GPS work base on signal strength and GPS satellite signals are weak (when compared to say cellular phone signals), so it doesn't work as well indoors, underwater, under trees, etc. Furthermore, GPS components available for WSNs application are costly. Besides, the highest accuracy requires line-of-sight from the receiver to the satellite: this is why GPS doesn't work very well in an urban environment. Moreover, the US DoD (dept. of defense) can, at any given time, deny the users use of the system (i.e. they degrade/shut down the satellites).

3.4 Evaluation of Different Localization Techniques with UWB

Currently, UWB technology is used widely for the localizing application especially in indoor environments. In order to employ this technology, different positioning algorithms have been developed in which position information is extracted from radio signals traveling between the reference nodes and target nodes in addition to the position information of the reference nodes. Until now, there are several positioning algorithms have been proposed. However, interestingly, researchers are also using a new approach named hybrid algorithm, where joint algorithms such as TOA-TDOA, AOA-TOA are used. In this section, we give a detailed review of these algorithms for UWB indoor positioning. A summary of UWB positioning algorithms is presented in Table 3.1 [24].

Tableau 3.1: Comparison of UWB systems

No.	Authors	Year	Algorithm	Environment	Details
1	Krishnan et al. [26]	2007	TDOA	LOS, NLOS	Used multi-cell implementation to cover large

					spaces, using Chan's method to provide an accurate estimate of the mobile tag's position within each cell. A heuristics-based approach was used to improve the accuracy at the boundaries.
2	Ch'oliz et al. [25]	2011	TOA	LOS, NLOS	Compared the performance of impulse radio (IR) UWB indoor tracking systems using different parametric and non-parametric algorithms such as weighted least square with multidimensional scaling (WLS-MDS), trilateration, least square with distance contraction (LS-DC), particle filter (PF), and extended kalman filter (EKF).
3	Pittet et al. [27]	2008	AOA,TDOA	NLOS	Combined UWB positioning with micro electro mechanical

					sensors (MEMS) inertial sensors in an extended Kalman filter to improve positioning and navigation performance.
4	Shahi et al. [28]	2012	AOA,TDOA	LOS,NLOS	Developed a UWB positioning system for material and activity tracking in indoor construction projects and studied the effect of construction materials on performance.
5	McCracken et al. [29]	2013	RSS	NLOS	Presented a device free positioning system that uses UWB radios together with RSS sensors to localize and track people

					through a building.
6	Wang and Zhang [30]	2014	TOA, AOA	NLOS	Used sparse representation framework for joint estimation of TOA and AOA.
7	Perrat et al. [31]	2015	TOA, TDOA	LOS	Used Ubisense for real-time positioning of wheelchair athletics.
8	Jiang et al. [32]	2012	TOA, RSS	LOS, NLOS	Proposed a new circuit to fully integrate a non-coherent IR-UWB transceiver, which rectified the baseband pulses and provided the digitized data to the digital baseband of the receiver.

9	Jiang et al. [33]	2013	TOA/TDOA	LOS	Presented a fast three dimensional node UWB positioning system that uses a modified propagator method for time delay estimation and a 3D Chan algorithm for position determination.
10	Zhang et al. [34]	2010	TDOA, RSS	NLOS	Presented a new non coherent UWB indoor positioning system with millimeter range accuracy.

Following up the table 3.1 we can see that different researchers established different localization algorithms with UWB technology. Such as in [34] and [27] authors proposed a hybrid localization technique based on TDOA-RSS and AOA-TDOA. Moreover, in both situation authors induct UWB technology to improve the rate of precision. In addition, most of the research has been conducted based on indoor and outdoor environment. Therefore, there is still a big gap left to employ those techniques in the harsh environment like an underground mine. Therefore, in our research we try to overcome this limitation and to evaluate the time base approach for localization in underground mine.

CHAPITRE 4

OUR APPROACH, SIMULATION AND RESULTS

A description about different localization methods, their advantages and disadvantages as well as their compliance with UWB technology has been introduced in chapter three. Following up the discussion, we fix that our research will be conducted using time base localization approach. So, in this chapter, we will discuss about our approach, simulation process, channel model and result analysis.

4.1. Overview of Localization

In this section, we will present the simulation process. In the appendix A, we have given the necessary function files; those have been used during the simulation. In our simulation, we have use time of arrival (TOA) and time difference of arrival of (TDOA) algorithm separately in order to evaluate and examine the performance in different situation. To perform the simulation, the anchor nodes are positioned in the network in such a way, where all nodes maintain equal distance from each other. Figure 4.1 describes the positional patterns of the anchor node, whereas

$$Node\ 1 = Node\ 2 = Node\ 3 = Node\ 4 = i$$

In order to simulate the positioning scheme involving these nodes, it is necessary to establish a UWB-based network from scratch. Each of the nodes needs to be able to transmit and receive UWB signals. In addition to transmitters and receivers, a channel model has been simulated in order to achieve a results that is as realistic as possible.

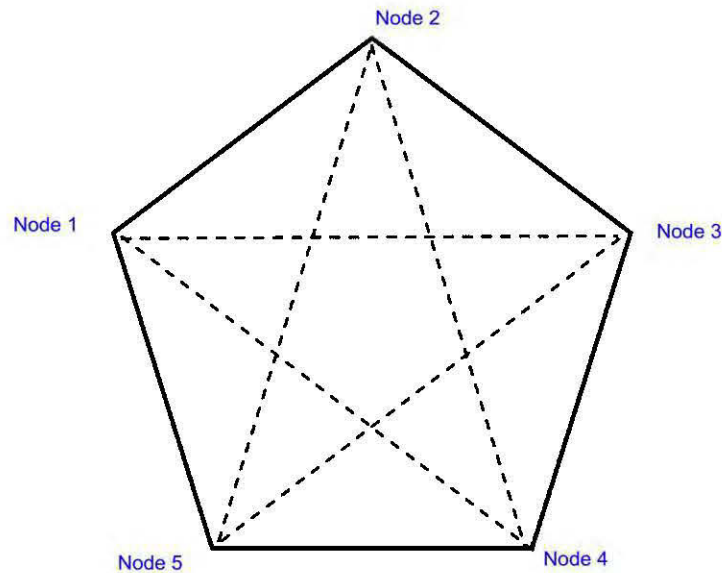


Figure 4.3: Anchor nodes position patterns.

The simulation of the UWB network is based on a physical layer where PPM modulation is used in addition to TH, in order to allow multiple access. As a channel model we have used UWB indoor channel model proposed by the IEEE 802-15-SG3a committee, described in section 4.2. Moreover, in the receiver section we have used RAKE receiver that exploits the reflections of the signal and thus makes a better detection than a regular correlation-based receiver, whereas it introduces the realistic estimate according to [38].

At the beginning, we ran our simulation based on in TOA algorithm, where we have measured the positioning error as root mean square (RMS) error. Then we ran our simulation following TDOA algorithm and observed the delay effect due to different channel parameter's effect. To justify our simulation work, we have used two different solutions (Nanotron and Decawave) to perform practical measurement. Both practical and simulation results show the remarkable co-relation about a delay effect in time base approach. The simulation was performed in MATLAB R2016a student version

software. At the end, in Appendix section, important functions, those that have been used in the simulation, are introduced.

4.2. Channel model

Following the measurement of broadband, the amplitude of a multipath fading follows the log normal or Nakagami distribution rather than the Rayleigh distribution, even though they show the same phenomenon of clustering in the Saleh-Valenzuela (S-V) channel model [36].

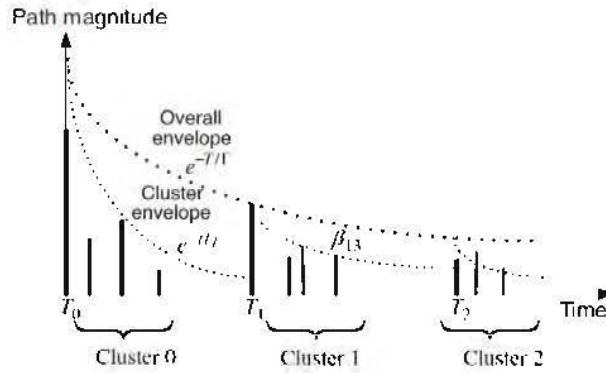


Figure 4.2: Saleh-Valenzuela channel model [37].

The S-V model is established in the observation, where multipath contributions generated by the same pulse arrive at the receiver into the cluster. The time of cluster arrival is modeled as a Poisson arrival process with rate Λ .

$$p(T_n|T_{n-1}) = \Lambda e^{-\Lambda(T_n - T_{n-1})} \quad (4.1)$$

Where T_n and T_{n-1} are the time of arrival of the n th and $(n-1)$ th clusters respectively. Within each cluster, subsequent multipath contributions also arrive according to a Poisson process with rate λ

$$p(\tau_n|\tau_{(n-1)k}) = \lambda e^{-\lambda(\tau_n - \tau_{(n-1)k})} \quad (4.2)$$

Based on the result obtained in July 2003, the channel modelling subcommittee of study group IEEE 802.15.SG3a proposed an UWB indoor multipath channel model. As a consequence, the channel impulse response of this model is represented by [37]:

$$h(t) = X \sum_{n=1}^N \sum_{k=1}^{K(n)} \alpha_{nk} \delta(t - T_n - \tau_{nk}) \quad (4.3)$$

Where X is a log normal variable representing the amplitude gain of the channel, N is the number of observed cluster, $K(n)$ is the number of multi path contributions received within the n th cluster, α_{nk} is the coefficient of the K th multi-path contribution of the n th cluster, T_n is the time of arrival of the n th cluster and τ_{nk} is the delay of the K th multi path contribution within the n th cluster.

According to the channel impulse response presented in eq. (3), the parameters of the model are defined by [37]:

- The cluster average arrival rate Λ .
- The pulse average arrival rate λ .
- The power delay factor Γ for cluster.
- The power delay factor γ for pulse within a cluster.
- The standard deviation σ_ξ of the fluctuation of the channel coefficient for the clusters.
- The standard deviation σ_ζ of the fluctuation of the channel coefficient for pulse within each cluster.
- The standard deviation σ_g of the channel amplitude gain.

Table I shows the list of parameters for different environment scenarios as defined by IEEE 802.15.SG3a [37].

Tableau 4.1: IEEE UWB channel model

Parameter	Case LOS (0-4m)	Case NLOS (0-4m)	Case NLOS (4-10m)	Case NLOS (Extreme)
Λ (1/ns)	0.0233	0.4	0.0667	0.0667

λ (1/ns)	2.5	0.5	2.1	2.1
Γ	7.1	5.5	14	24
γ	4.33	6.7	7.9	12
σ_{ξ} (dB)	3.3941	3.3941	3.3941	3.3941
σ_{ζ} (dB)	3.3941	3.3941	3.3941	3.3941
σ_g (dB)	3	3	3	3
Target Channel Characteristics	Case LOS (0-4m)	Case NLOS (0-4m)	Case NLOS (4-10m)	Case NLOS (Extreme)
Mean excess delay (nsec) ($\bar{\tau}$)	5.05	10.38	14.18	
RMS delay (nsec) (σ_{τ})	5.28	8.03	14.28	25
NP10dB			35	
NP (85%)	24	36.1	61.54	
Model Characteristics	Case LOS (0-4m)	Case NLOS (0-4m)	Case NLOS (4-10m)	Case NLOS (Extreme)
Mean excess delay (nsec) ($\bar{\tau}$)	5.05	10.38	14.18	
RMS delay (nsec) (σ_{τ})	5.28	8.03	14.28	25
NP10dB			35	
NP (85%)	24	36.1	61.54	
Channel Energy mean (dB)	-0.4	-0.5	0.0	0.3

Channel Energy std (dB)	2.9	3.1	3.1	2.7
-------------------------------	-----	-----	-----	-----

4.3. Simulation results

4.3.1 Localization via TOA

At the initial stage of our research work, we have performed a simulation following TOA algorithm, where we have observed the positioning error. In order to measure the positioning error, we use root mean square (RMS) error. In addition, the mathematical expression of the RMS error is expressed as below:

$$RMSE = \sqrt{(x_{practicle} - x)^2 + (y_{practicle} - y)^2} \quad (4.4)$$

The simulation has been performed over 15 meters of distance. In the LOS simulation, we have used case LOS (0-4m) channel parameters for 0 to 4m of distance, where's we have used case LOS(4-10m) for 4m to 10m of distance. However, for the NLOS we have used case NLOS (4-10m) channel parameters [cf. Table 4.1]. Figure 4.3 shows the positioning error curve for TOA algorithm. It shows that for both LOS and NLOS the error curve is getting higher. Furthermore, the rate of error is higher for NLOS than LOS. This indicate that the delay is getting higher with distance, which also indicate the higher error. However, there are some other factors that are important during localization such as transmitter power and frequency value. If the transmitter power is low localization experience more error in order to measure the real distance of unknown node. During simulation, we used different transmitter power, such as: -20 dB, -15 dB, -10 dB, -5 dB. However, we have observed higher efficiency for – 5 dB than others. Additionally, for 10 meters of distance in NLOS we observe 2.6 meters of error for -5 dB, where for same distance we observe 4.3 meters of error for -10 dB.

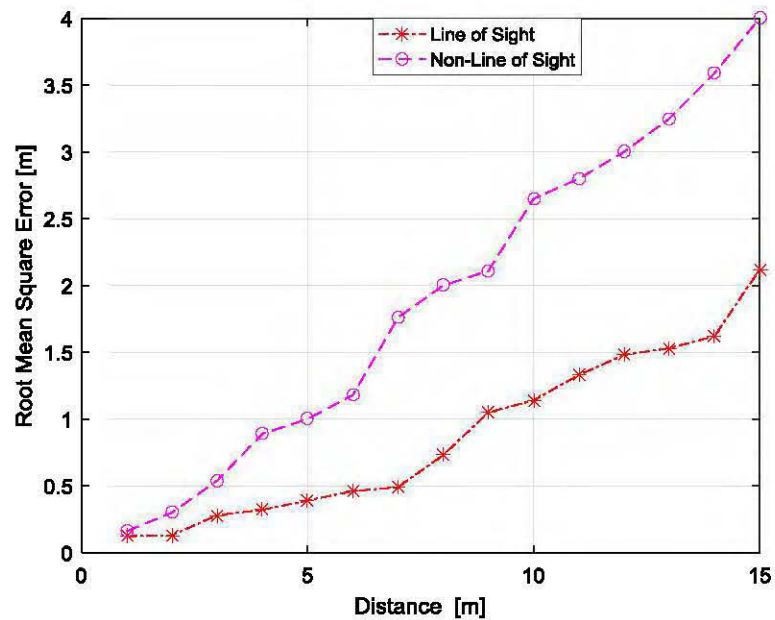


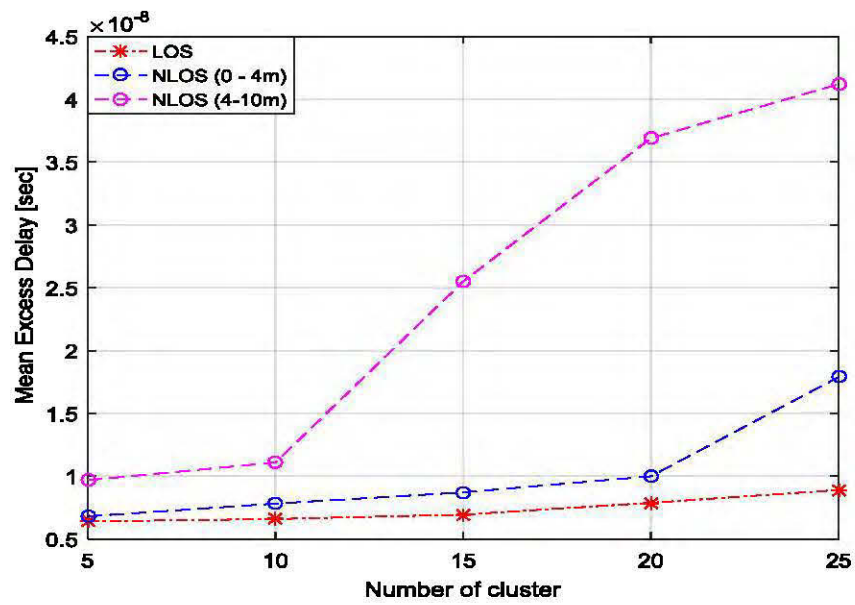
Figure 4.3: Positioning error for TOA.

4.3.2 Localization via TDOA and channel parameters effect:

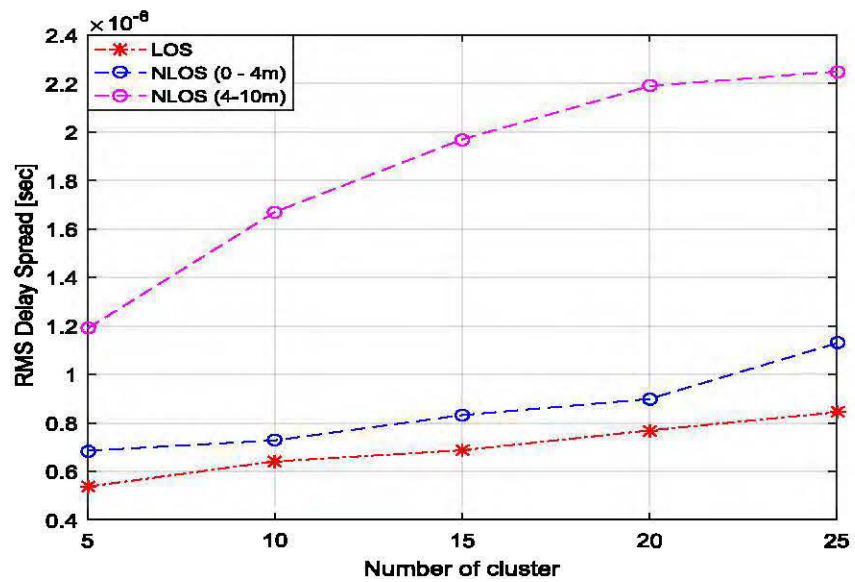
From the previous section, we have a basic idea about localization error. However, it does not show the real effect in terms of delay (time base approach) and the effect of channel parameters. That's why, in the second term of our research, we performed a descriptive analysis, where we show the effect of different UWB channel parameters, for instance: cluster arrival rate and ray arrival rate in time base localization. Then, we extract the information about RMS delay spread as well as mean excess delay for line of sight (LOS) and non-line of sight (NLOS) Scenarios in indoor environments. However, this time we used TDOA instead of TOA. However, although NLOS is divided into three cases, we count the two cases while the NLOS case extreme is unused. The two cases: 0 to 4m and 4m to 10m denoted respectively by NLOS1 and NLOS2 (cf. Table 4.1). However, for the LOS we have used case LOS (0-4m) channel parameters for 0 to 4m of distance. On the other hand, we have used case LOS(4-10m) for 4m to 10m of distance. For each scenario in the first stage, we change the number

of clusters and kept other parameters unchanged. In the next stage, we did the inverse operation by changing the number of rays and kept other parameters unchanged.

- a. **Analysis According to the Number of Clusters:** For both LOS and NLOS scenarios, figure 4.4 shows the effect of changing the number of clusters in TDOA UWB localization. During simulations, the parameter λ , the ray arrival rate, is fixed to 2.5, 0.5 and 2.1 for LOS, NLOS1 and NLOS2 respectively. Figure 4.4(a) shows that the rate of mean excess delay increases remarkably with the number of clusters for all the cases, where for NLOS2 case, the delay rate is relatively higher than NLOS1 and LOS case. For the mean excess delay, a maximum of 25 clusters was reached for NLOS1 and NLOS2 cases in 17 nsec and 42 nsec respectively. On the other hand, figure 4.4(b) shows the clusters effect over RMS delay spread. The delay effect is comparatively lower than it is for the mean excess delay, for the same number of clusters. Even though, the maximum RMS delay spread is displayed in NLOS2 case, the delay changes steadily for all these cases over the clusters.
- b. **Analysis According to the Number of Rays:** During the performance analysis of the ray's effect on TDOA UWB localization for all scenarios, the parameter λ , the cluster arrival, was fixed to 0.02, 0.4 and 0.06 for LOS, NLOS1 and NLOS2 respectively. Figure 4.5 shows the number of ray effects on the mean excess delay and the RMS delay spread. Figure 4.5(a) shows that with the number of rays, the mean excess delay is increasing rapidly. For instance, in LOS scenario for 300 rays, the value of mean excess delay is around 6.3 nsec, while for 500 rays, the delay reaches up to 8.2 nsec. For NLOS1 case, the mean excess delay is relatively higher and reaches 12 nsec, though for NLOS2 the delay reaches 42 nsec. On the other hand, in figure 4.5(b), the effect of ray numbers over RMS delay spread is comparatively higher than mean excess delay, such as in LOS scenario for 300 rays, the rms delay spread reaches 7 nsec, while for 500 rays the rms delay spread reaches 9 nsec.

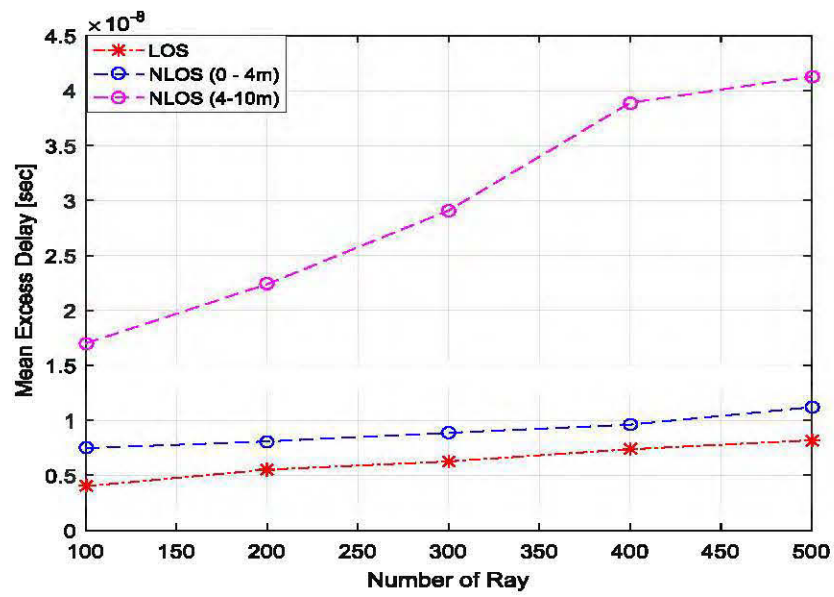


(a)

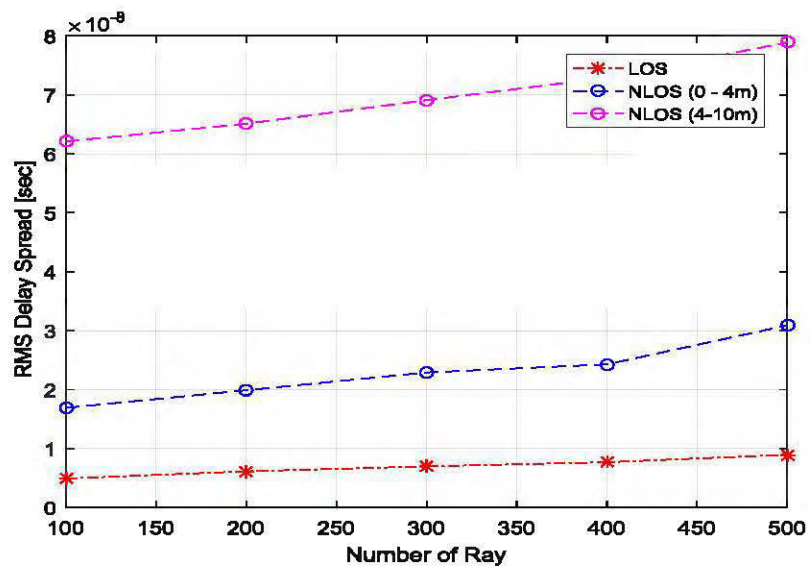


(b)

Figure 4.4: (a) and (b) represents the effect of cluster number changes over mean excess delay and RMS delay spread



(a)



(b)

Figure 4.5: (a) and (b) represents the effect of ray number changes over mean excess delay and RMS delay spread.

After observing the position error for TOA localization and channel parameter effects for TDOA localization, we conduct the experimental analysis to justify our experimental results as well as to identify the nature and effectiveness for time base localization in indoor and rush environment like underground mine.

4.4. Measurement Results

4.4.1 Indoor Scenario

The indoor measurements were conducted, as illustrated by fig 4.6 and 4.7, in partly open intermediate floor of the building to the double-height ceilinged floor below the university campus (UQAT). The wall is composed of wood and metal, where the floor is made of concrete. This area is divided in two sections: Line of sight (LOS) and Non line of sight (NLOS). In order to perform measurement, we have used two different environment scenarios for Nanotron and Decawave respectively. Figure 4.6 shows the environment scenarios for Nanotron measurement. In LOS area, 6 to 11 meters are introduced as obstructed line of sight (OLOS) for being surrounded by metallic cabinets, tables and glasses. Further, the NLOS measurement area is divided into two sections, where first 2 meters are defined as LOS and the other 13 meters are defined as NLOS.

Figure 4.7 shows the environment scenarios for Decawave measurement, where for NLOS measurement area the first 6 meters are defined as LOS and the rest (4 meters) are considered as NLOS. For all the measurements, the anchor sensors were placed at the height of 1 meters from the floor. For each technology (UWB and 2.4 GHz) we used three anchor nodes and one unknown node that needs to be localized. In total, 15 measurements have been carried out using directional UWB patch antenna and omnidirectional 2.4GHz antenna.



Figure 4.6: Measurement Scenarios for Nanotron.



Figure 4.7: Measurement Scenarios for Decawave.

4.4.2 Underground mine scenario

The measurements for the underground mine environment has been performed in Cité de l'Or ("The City of Gold"). That is located in Val-d'Or, in the Abitibi-Témiscamingue region of Quebec, Canada. In 1923, the gold deposit was discovered and in 1935, the mine came in operation. However, in 1985, it was exhausted and closed. Therefore, since 1995 it has been operating as a place where people can see what gold mining was like, by touring the underground Lamaque Gold Mine and the Bourlamaque historic mining village. Bourlamaque was declared a provincial historic site in 1979 [39] and a National Historic Site in 2012 [40].

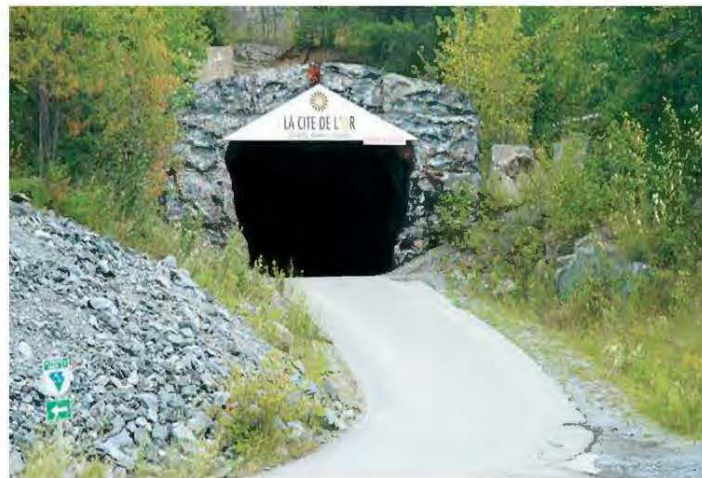


Figure 4.8: Cité de l'Or mine, val-d'Or entrance.

We have performed our measurements 100 meters from the ground level at FOREUSE "JUMBO" point (c.f. fig 4.9) in the circular and rectangular cross-sectional tunnel of Cité de l'Or mine. Figure 4.10 describes the scenarios of the mine tunnels inside. The side walls and top wall of the tunnel are rocky. However, the ground of the tunnel is sweaty and temperature is contained around 15°C. For both NLOS (non-line of sight) and LOS (line of sight) environment, the measurements have been performed over 15 meters of distance. Figure 4.11 and 4.12 describe the LOS and NLOS

environment. The NLOS environment, as described in figure 4.12, is divided into two sections, where first 3 meters are defined as LOS and the other 12 meters are defined as NLOS.

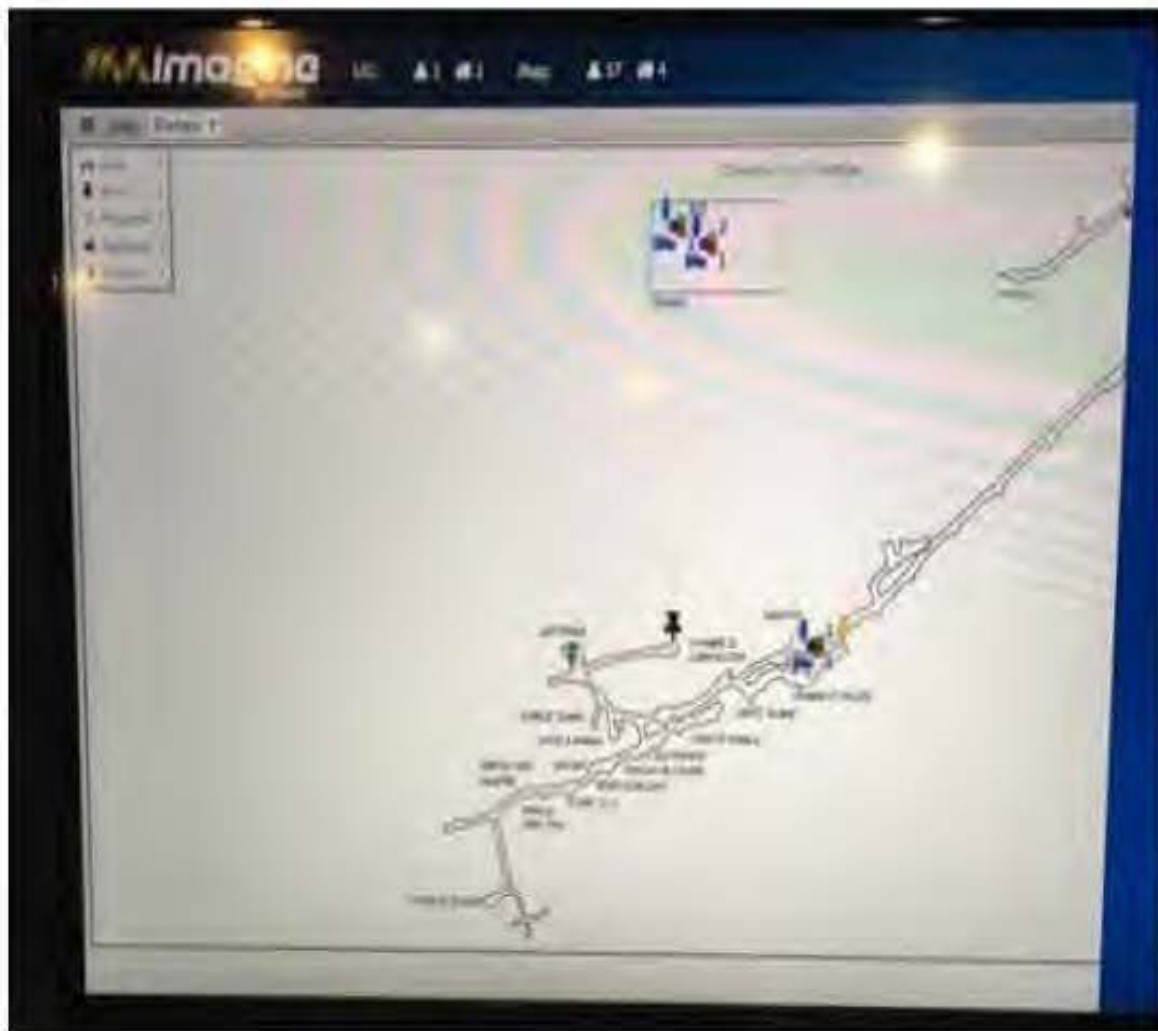


Figure 4.9: Cité de l'Or mine Map.



Figure 4.10: Setup measurement inside mine tunnel.



Figure 4.41: Measurement Scenario for LOS.



Figure 4.52: Measurement Scenario for NLOS.

4.4.3 Used sensor

- a. **Nanotron Solution:** The German Company Nanotron brings out a real time locating system (RTLS) for localization called Nanotron solution. It offers a positioning infrastructure that includes the anchors (source nodes) and the tags (target nodes). Two good features of their technology are a LiPo embedded battery for the tags and adjustable signal power. The main drawback of the Nanotron technology is that uses the chirp spread spectrum physical layer technology instead of using the impulse radio; that is why the accuracy of their technology is significantly weaker compared to Ubisense and Decawave. The Nanotron real time location (RTL) technology's accuracy is 1 m to 3 m. The positioning approach used by Nanotron is TOA. Nanotron provides a test kit which includes 8 stationary nodes, 5 tags and the needed software. The price of this package with educational discount is about 5,000.00 CAD. In our work, we used Nanotron solution to estimate distance from TOA for UWB and 2.4 GHz technology. Thus, we used

Swarm bee ER module for UWB and Swarm bee LE module for 2.4 GHz. The operating band of swarm bee ER is 3.5 to 6.5 GHz, where the swarm bee LE module works between 2.4 and 2.4835 GHz ISM frequency band [41].



Figure 4.63: Nanotron Sensor. [46]

- b. Decawave Solution: The Decawave Company has an IEEE802.15.4a compliant sensor which is able to perform positioning by TOA or TDOA approach. The producer claims that the accuracy of this sensor working with 1.3GHz bandwidth is ± 10 cm. According to the producer's website, the key benefits of this sensor, called DW1000, are precise ranging, long LOS and NLOS communication range (up to 290m), high data rate (up to 6.8 Mbit/s) and low power consumption. The EVB1000 Evaluation Board is a complete device including the DW1000IC, ARM programmable processor, LCD, USB connection and antenna. The dimensions of the EVB 1000 are 7×7 cm excluding the off-board antenna and the range of the center frequency of six available UWB channels is 3.5 to 6.5 GHz. The

Decawave's device is more suitable for research and development because it is programmable, smaller and it has embedded LCD and USB connections. The price of the evaluation kit is 606.67 USD. The price of the module, which includes transmitter IC and integrated antenna, is about 50 CAD and the price of a single transmitter IC is 20 CAD. Moreover, Decawave solution is supported by four different modes of operation along with data rate and frequency channel. Additionally, these four operational modes are divided into short and long frame. Table 4.2 shows the details of operational mode.

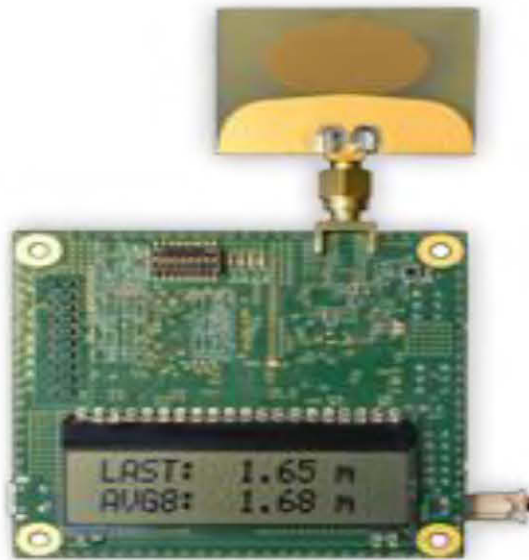


Figure 4.74: Decawave Sensor. [45]

Tableau 4.2: Operational Mode

Mode	Channel	Data rate
L2 (long frame)	2 (4 GHz)	110kbps
L5 (Long frame)	5 (6.5 GHz)	110kbps
S2 (short frame)	2 (4 GHz)	6.8 Mbps
S5(short frame)	5(6.5 GHz)	6.8 Mbps

4.5. Measurement Results

4.5.1. Indoor scenario

- a. Using Nanotron: Following the described scenario in section 4.4, we conducted the indoor measurement using Nanotron. The measurement was conducted using both the 2.4 GHz and UWB solutions of the Nanotron solution. In order to make a meaningful comparison we also used 2.4 GHz technology during measurement with UWB. 2.4 GHz technology is the allocated frequency band for IEEE 802.11WLAN standard that was released in June 1997. Upon the application, this technology works with different data rate such as 11, 54 or 108 Mbps for 50 to 100 meters of distance. Even though this technology works mostly with RSSI, it is also partially employed with TOA, TDOA and AOA. However, Figure 4.15 and 4.16 shows the results for LOS and NLOS using Nanotron solutions. Figure 4.15 shows that root mean square error in LOS area is increasing gradually with the actual distance for both UWB and 2.4 GHz. After 10 m, the error for 2.4 GHz is getting relatively lower than UWB and reaches from 1.5 m to 15 m actual distance. For UWB, the curve behavior continues to increase after 10 m. In figure 4.16, for the NLOS scenario, the error curve increases gradually with actual distance for both technologies and is higher comparatively to the LOS scenario. Nevertheless, at a distance around 10

meters, we can see an intersection point from where the level of error for 2.4 GHz is comparatively lower than UWB. Therefore, our experiment shows that UWB technology performs better than 2.4GHz and the distance error is remarkably lower for 0 to 11 meter's distance in LOS environment along with 0 to 10 meters for NLOS environment. On the other hand, for 2.4 GHz, even though for the short range 0 to 11 meters for LOS and 0 to 10 meters for NLOS the rate of error is higher, beyond that this technology shows better performance than UWB. However, our work shows that UWB-TOA is more effective than 2.4GHz-TOA technique for short range in indoor environment.

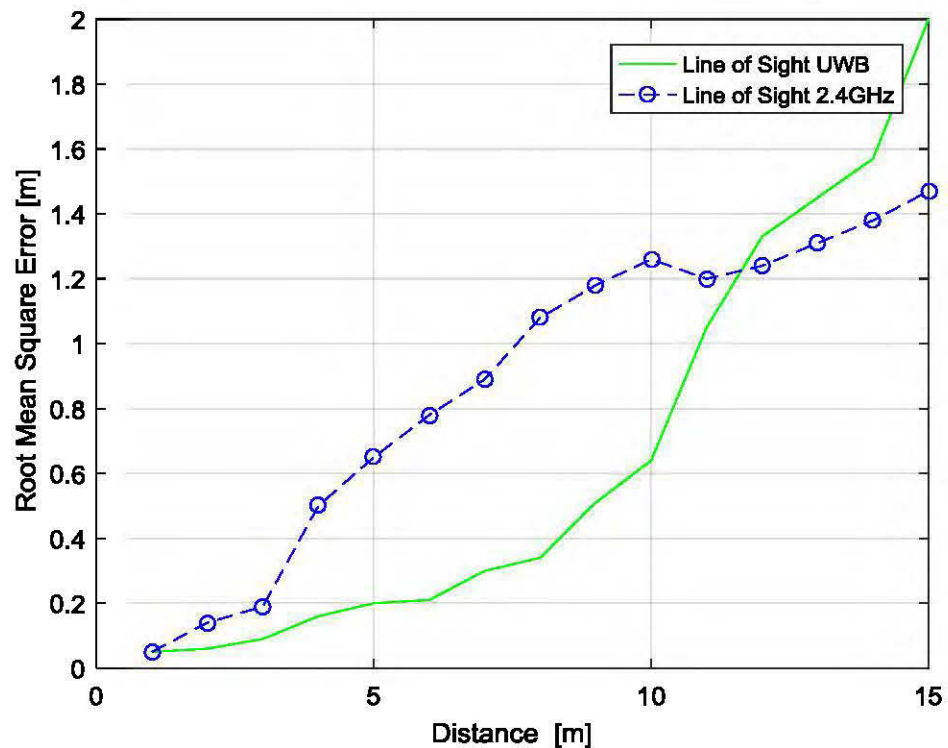


Figure 4.85: Measurement using Nanotron for LOS.

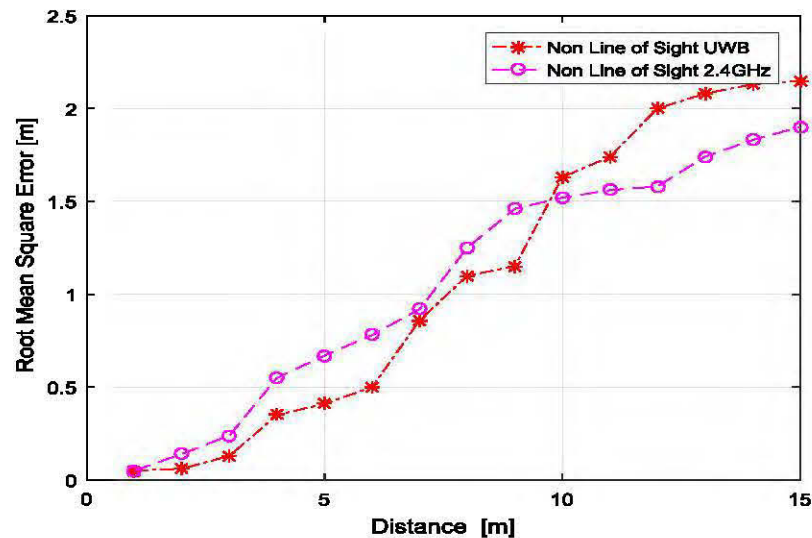


Figure 4.96: Measurement Using Nanotron for NLOS.

- b. Using Decawave [41]: Similarly, following the described scenario in section 4.4, we conducted the indoor measurement using Decawave Solution. To conduct the measurement, we used Decawave UWB solution. Apart from that, the Decawave solution shows the channel impulse response in real-time during the measurement, while figure 4.17 and 4.18 shows the channel impulse response for LOS and NLOS scenarios in indoor environments, where the blue line is the computed magnitude values. The graphic also indicates with a vertical orange line where the DW1000 finds the leading path. In normal operation of the DW1000 there is no need to access this channel impulse response data, which is quite a lot of data, doing so will slow down system responsiveness. The hardware reported RX timestamp is accurate and is all that is needed. Figure 4.19 and 4.20 show the measurement results (RMS error) for Decawave solution against simulation results. However, the measurement results are a bit different than Nanotron. Even though the rate of error is getting higher with the distance, the average rate of error for both LOS and NLOS is relatively low. For

example, for 10 meters in LOS we observed distance error for Nanotron UWB module is 0.6m, where for Decawave its 0.5m. Further, for 10 meters in NLOS we observed distance error for Nanotron UWB module is 1.5m, where for Decawave its 0.8m. Additionally, for 10 meters of distance, the distance error reach to 0.7m and 0.8m for LOS and NLOS respectively, which indicate the higher accuracy of Decawave. Nevertheless, the rate of error is relatively lower. This lower rate of error shows the effectivity of IR UWB technique in the terms of accuracy.

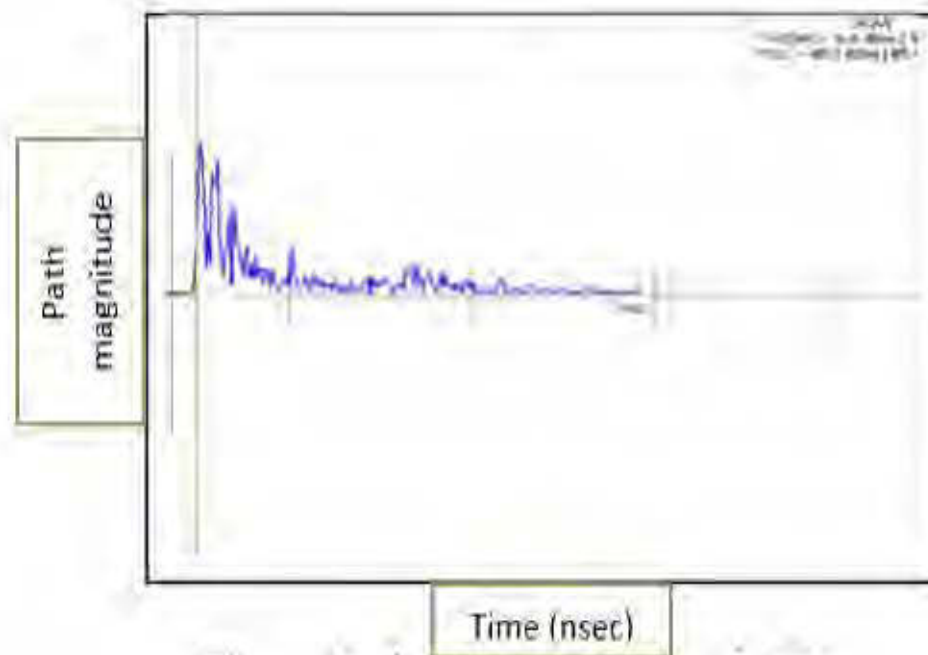


Figure 4.17: Channel Impulse Response for LOS.

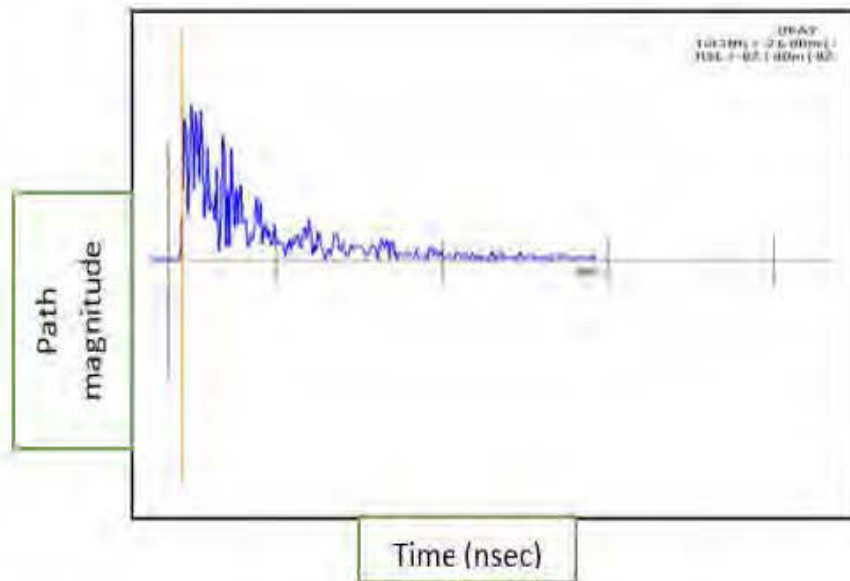


Figure 4.108: Channel Impulse Response for NLOS.

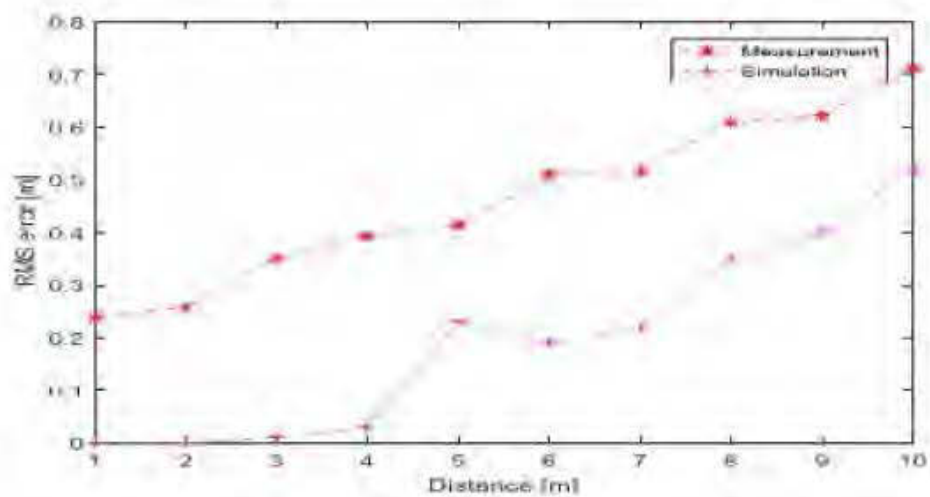


Figure 4.119: Simulation and measurement using Decawave for LOS.

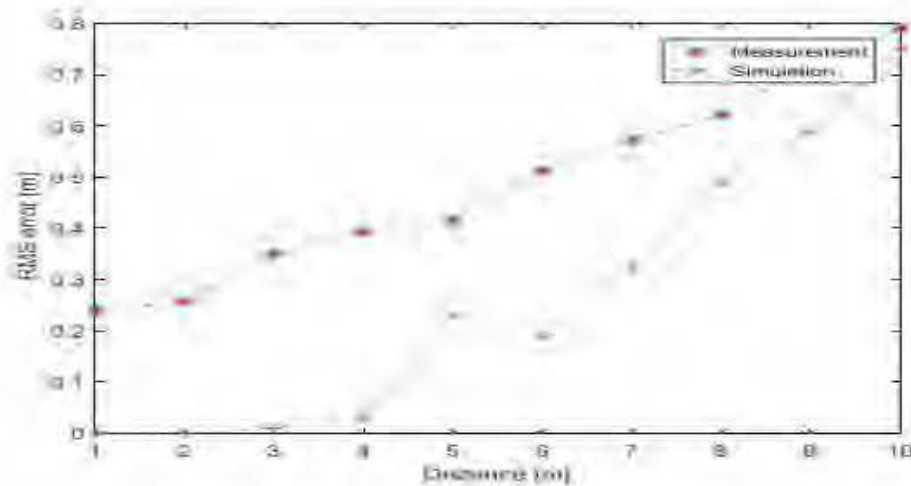


Figure 4.20: Simulation and measurement using Decawave for NLOS

4.5.2 Underground mine scenario

Following the described scenario in section 4.4, we conducted the Underground mine measurement using Decawave only. The measurement was conducted using UWB solution of Decawave. In addition, the measurements have taken four operational modes (cf. Table 4.2). Figure 4.21 and 4.22 shows the measurement results in underground mine for both LOS and NLOS scenarios. Following figure 4.21, the positioning error for all operational modes in LOS has been shown. It is clear that with the distance, the positioning error is getting higher. However, the rate of errors is different for each mode. The minimum error that was observed for L2 is 0.3 meters, where S5 shows the maximum rate of error at 0.97 meters. On the other hand, for the NLOS following figure 4.22, the rate of errors is also different for each operation mode, though all errors follow up each other closely. The minimum error for NLOS is 1.71 and it is showing for the L5 mode, where the maximum error is 2.09 and it shows for S5 mode.

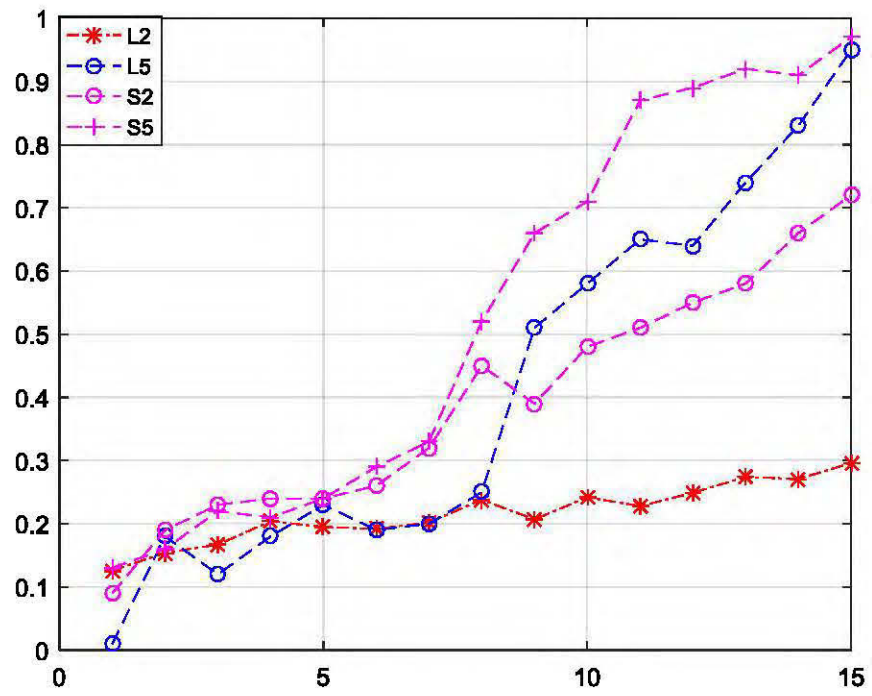


Figure 4.21: Measurement using Decawave for LOS (Underground mine).

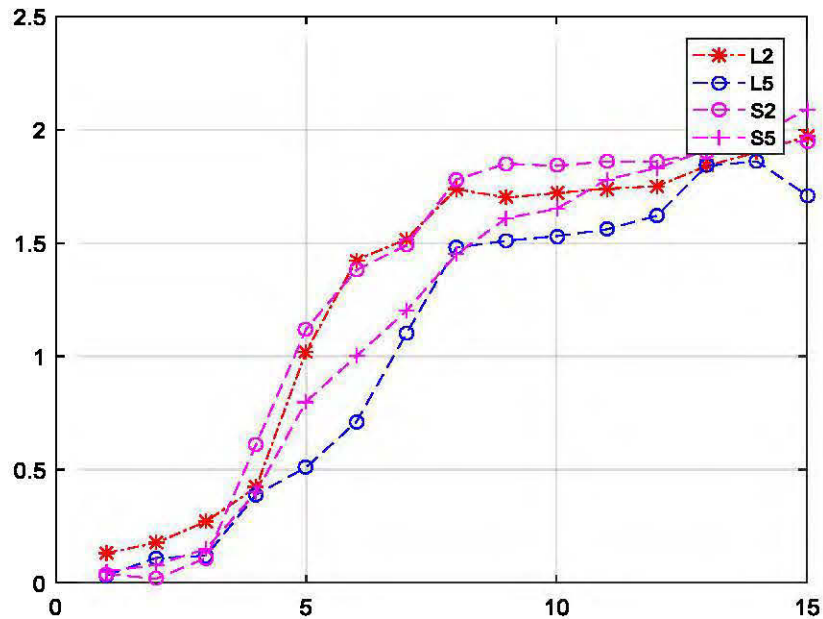


Figure 4.22: Measurement using Decawave for NLOS (Underground mine).

The frame intuition has been played a big role in localization performance for underground mine even after having same frequency band. It is because if a MAC frame is longer than a threshold level, it will split the longer frame into multiple short frame and concentration. Moreover, for the fragmentation each fragment acknowledge individually and not need to go through the channel contention for the other fragments in the same frame. That gives the better bandwidth efficiency for longer frame than shorter frame.

In addition, because of this reason, during the measurement, we found the same reflection for large frame L2, L5 over short frame S2, S5.

CONCLUSION

A time base tracking and positioning scheme has been presented in this research work, where we have performed the simulative and practical work respectively. In the beginning, we performed a simulation work using time of arrival algorithm. Besides ultra-wide band (UWB) technology has been used. In the result, we have seen that, the higher delay causes higher positioning error (figure 4.3). However, the error change or vary with the change of transmitting power and frequency. In order to justify this simulation work, we have conducted an experimental work using Nanotron solution in indoor environments. We also used two different solutions of Nanotron such as 2.4 GHz and UWB.

In essence, beside justification our experimental work also aims to propose the better technique for indoor localization as well as to establish a projectile threshold level for distance for both UWB and 2.4 GHz, in order to choose the best and efficient technology for localization. Besides, untill now, there is not enough experimental works that have been conducted to check the operation range for UWB and 2.4 GHz technology. That's why, in our research, we tried to overcome those issues. Experiment shows that for LOS, in a range of 0 to 11 meters, UWB is the best option and above that range 2.4 GHz is the best option. On the other hand, for NLOS in a range of 0 to 10 meters UWB is the best technology and beyond that range, 2.4 GHz is performing better for localization.

In the next stage, we tried to evaluate the delay effect in localization with more details, where we describe the different channel parameter effects in the term of delay. The channel parameters include cluster arrival rate, ray arrival rate, etc. To perform it, we run a simulation again, but using TDOA UWB mechanism and measure different delay effects like root mean square (RMS) delay spread & mean excess delay. Where

the results (fig. 4.4 and 4.5) shows the remarkable delay effect for different channel parameters.

Again, to validate this work we have performed an experimental measurement in indoor environments using Decawave UWB solution (figure 4.19 and 4.20). Results show the channel impulse response, which describes the effects number of clusters and rays can have during the measurements. Beside, we also performed the same measurements in the underground mine environment. The results show the higher accuracy for TDOA-UWB in indoor and underground mine environment as well as the channel parameters effect.

By observing and analyzing all the results, we may conclude that, the time base localization with UWB technology is promisingly good and an accurate addition for localization. That might bring out a revolutionary change in terms mechanism for existing locating system. Though most of the commercial for localization receiving signal strength, the time base mechanism (TOA/TDOA) with UWB technology has also higher possibility in near future to change trend and to bring out a better and more accurate results for tracking and positioning.

RÉFÉRENCES

- 1 M. M. Zanjireh, H. Larijani, "A Survey on Centralised and Distributed Clustering Routing Algorithms for WSNs", IEEE 81st Vehicular Technology Conference. Glasgow, Scotland: IEEE. Spring 2015
- 2 <http://www.silabs.com/documents/public/white-papers/evolution-of-wireless-sensor-networks.pdf>
- 3 D. Tse et P. Viswanath, Fundamentals of wireless communication: Cambridge university press, 2005.
- 4 A. Qandour, D. Habibi, and I. Ahmad, "Applied application of sensor networks in underground mines," in Networking, Sensing and Control (ICNSC), 2012 9th IEEE International Conference on, 2012, pp. 256-260.
- 5 <http://www.nytimes.com/2007/08/17/us/17mine.html>
- 6 M.K. Jain, "Wireless Sensor Networks: Security Issues and Challenges", International Journal of Computer and Information Technology, vol. 2, no. 1, 2011, pp. 62-67.
- 7 W. W. Dargie and C. Poellabauer, Fundamentals of wireless sensor networks: theory and practice: John Wiley & Sons, 2010.
- 8 Xuemin (Sherman) Shen, Weihua Zhuang, Hai Jiang, and Jun Cai, "Medium access control in ultra-wideband wireless networks," IEEE Transactions On Vehicular Technology, VOL. 54, NO. 5, pages 1663-1677, September 2005.
- 9 I. G. Zafer Sahinoglu, Sinan Gezici. Ultra-wideband Positioning Systems: Theoretical Limits, Ranging Algorithms, and Protocols. Cambridge University Press, October 6, 2008.
- 10 Arne Svensson, Arumugam Nallanathan, and Ahmed Tewfik, "Ultra-Wideband Communication Systems: Technology and Applications", EURASIP Journal on Wireless Communications and Networking, Volume 2006, Article ID 16497, Pages 1–3.
- 11 Maria-Gabriella Di Benedetto and Guerino Giancola. Understanding Ultra Wide Band. Radio Fundamentals. Prentice Hall PTR, 2004.
- 12 J. Ni, D. Arndt, P. Ngo, C. Phan, K. Dekome, and J. Dusl, "Ultrawideband Time-Difference-Of-Arrival High Resolution 3D Proximity Tracking System," in IEEE/ION Position, Location and Navigation Symposium, 2010, pp. 37-43.

- 13 P. Pannuto, "Ultra-wideband and indoor localization," présenté à Proceedings of the 3rd
Workshop on Hot Topics in Wireless, New York City, New York, 2016.
- 14 http://www.signal.uu.se/Research/PCCWIP/Visbyrefs/Svensson_Visby04.pdf
- 15 http://ids.nic.in/tnl_jees_mar_2010/uwb.htm
- 16 W. Dargie et C. Poellabauer, *Fundamentals of Wireless Sensor Networks: Theory and Practice*:
Wiley Publishing, 2010.
- 17 S. Yadav et R. S. Yadav, "A review on energy efficient protocols in wireless sensor networks,"
Wirel. Netw., vol. 22, pp. 335-350, 2016.
- 18 C. Wang et L. Xiao, "Sensor Localization under Limited Measurement Capabilities," *Netwrk. Mag.
of Global Internetwkg.*, vol. 21, pp. 16-23, 2007.
- 19 [1] T. Padois, M.-A. Gaudreau, O. Doutres, F. C. Sgard, A. Berry, P. Marcotte et F. Laville,
"Comparison of time domain noise source localization techniques: Application to impulsive noise
of nail guns," *The Journal of the Acoustical Society of America*, 2017.
- 20 P. Bahl and V. N. Padmanabhan, "RADAR: an in-building RF-based user location and tracking
system," in Proceedings IEEE INFOCOM 2000. Conference on Computer Communications.
Nineteenth Annual Joint Conference of the IEEE Computer and Communications Societies (Cat.
No.00CH37064), 2000, pp. 775-784 vol.2.
- 21 D. Niculescu and N. Badri, "Ad hoc positioning system (APS) using AOA," in IEEE INFOCOM
2003. Twenty-second Annual Joint Conference of the IEEE Computer and Communications
Societies (IEEE Cat. No.03CH37428), 2003, pp. 1734-1743 vol.3.
- 22 N.-q. Li and P. Li, "A Range-Free Localization Scheme in Wireless Sensor Networks," in 2008
IEEE International Symposium on Knowledge Acquisition and Modeling Workshop, 2008, pp.
525-528.
- 23 J.-Y. Lee and R. Scholtz, "Ranging in a dense multipath environment using an UWB radio link,"
Selected Areas in Communications, IEEE Journal on, vol. 20, pp. 1677-1683, 2002.
- 24 I. F. Akyildiz et E. P. Stuntebeck, "Wireless underground sensor networks: Research challenges,"
Ad Hoc Networks, vol. 4, pp. 669-686, 2006/11/01/ 2006.
- 25 A. Alarifi, A. Al-Salman, M. Alsaleh, A. Alnafessah, S. Al-Hadhrami, M. Al-Ammar et H. Al-
Khalifa, "Ultra Wideband Indoor Positioning Technologies: Analysis and Recent Advances,"
Sensors, vol. 16, p. 707, 2016.

- 26 Chóliz, J., Eguizabal, M., Hernandez-Solana, A., Valdovinos, A. Comparison of Algorithms for UWB Indoor Location and Tracking Systems. In Proceedings of the 2011 IEEE 73rd Conference on Vehicular Technology Conference (VTC Spring), Budapest, Hungary, 15–18 May 2011; pp. 1–5.
- 27 Krishnan, S.; Sharma, P.; Guoping, Z.; Woon, O. A UWB based localization system for indoor robot navigation. In Proceedings of the IEEE International Conference on Ultra-Wideband, ICUWB 2007, Singapore, 24–26 September 2007; pp. 77–82.
- 28 S. Pittet, V. Renaudin, B. Merminod et M. Kasser, "UWB and MEMS Based Indoor Navigation," *Journal of Navigation*, vol. 61, pp. 369-384, 2008.
- 29 A. Shahi, A. Aryan, J. S. West, C. T. Haas et R. C. G. Haas, "Deterioration of UWB positioning during construction," *Automation in Construction*, vol. 24, pp. 72-80, 2012/07/01/ 2012.
- 30 McCracken, M., Bocca, M., & Patwari, N. (2013, June). Joint ultra-wideband and signal strength-based through-building tracking for tactical operations. In *Sensor, Mesh and Ad Hoc Communications and Networks (SECON), 2013 10th Annual IEEE Communications Society Conference on* (pp. 309-317). IEEE.
- 31 F. Wang et X. Zhang, "Joint estimation of TOA and DOA in IR-UWB system using sparse representation framework," *ETRI Journal*, vol. 36, pp. 460-468, 2014.
- 32 B. Perrat, M. J. Smith, B. S. Mason, J. M. Rhodes et V. L. Goosey-Tolfrey, "Quality assessment of an Ultra-Wide Band positioning system for indoor wheelchair court sports," *Proceedings of the Institution of Mechanical Engineers, Part P: Journal of Sports Engineering and Technology*, vol. 229, pp. 81-91, 2015.
- 33 X.-y. Jiang, H.-s. Zhang et W. Wang, "NLOS error mitigation with information fusion algorithm for UWB ranging systems," *The Journal of China Universities of Posts and Telecommunications*, vol. 19, pp. 22-29, 2012/04/01/ 2012.
- 34 Jiang, Hong, Yu Zhang, Haijing Cui, and Chang Liu. "Fast three-dimensional node localization in UWB wireless sensor network using propagator method digest of technical papers." In *Consumer Electronics (ICCE), 2013 IEEE International Conference on*, pp. 627-628. IEEE, 2013.
- 35 C. Zhang, M. J. Kuhn, B. C. Merkl, A. E. Fathy et M. R. Mahfouz, "Real-time noncoherent UWB positioning radar with millimeter range accuracy: Theory and experiment," *IEEE Transactions on Microwave Theory and Techniques*, vol. 58, pp. 9-20, 2010.
- 36 D. Benedetto, *Understanding ultra wide band radio fundamentals*: Pearson Education India, 2008.

- 37 A. A. Saleh et R. Valenzuela, "A statistical model for indoor multipath propagation," *IEEE Journal on selected areas in communications*, vol. 5, pp. 128-137, 1987.
- 38 N. J. August, "Medium access control in impulse-based ultra wideband ad hoc and sensor networks," 2005.
- 39 <http://www.historicplaces.ca/>
- 40 Former Lamaque Mine and the Bourlamaque Mining Village National Historic Site of Canada. Directory of Federal Heritage Designations. Parks Canada. Retrieved 24 October 2013.
- 41 <https://www.decawave.com/support>
- 42 A. Fluerasu, N. Jardak, A. Vervisch-Picois et N. Samama, "Status of the GNSS transmitter-based approach for indoor positioning," *Coordinates Magazine*, vol. 7, 2011.
- 43 G. Cheng, "Accurate TOA-based UWB localization system in coal mine based on WSN," *Physics Procedia*, vol. 24, pp. 534-540, 2012.
- 44 E. Arias-de-Reyna et U. Mengali, "A maximum likelihood UWB localization algorithm exploiting knowledge of the service area layout," *Wireless personal communications*, vol. 69, pp. 1413-1426, 2013.
- 45 <https://www.decawave.com/products/trek1000>
- 46 http://nanotron.com/EN/PR_protect.php
- 47 G. Mao, B. Fidan et B. D. O. Anderson, "Wireless sensor network localization techniques," *Computer Networks*, vol. 51, pp. 2529-2553, 2007/07/11/ 2007.
- 48 C. Suwatthikul, W. Chantaweesomboon, S. Manatrinon, K. Athikulwongse et K. Kaemarungsi, "Implication of anchor placement on performance of UWB real-time locating system," *dans Information and Communication Technology for Embedded Systems (IC-ICTES), 2017 8th International Conference of*, 2017, pp. 1-6.

APPENDIX A

A. Evaluates the Power Delay Profile 'PDP'

```

% Evaluates the Power Delay Profile 'PDP'
% of a channel impulse response 'h' sampled
% at frequency 'fc'
%
% Programmed by Guerino Giancola
%

function [PDP] = cp0802_PDP(h,fc)

% -----
% Step One - Evaluation of the PDP
% -----

dt = 1 / fc;          % sampling time

PDP = (abs(h).^2)./dt % PDP

% -----
% Step Two - Graphical Output
% -----

Tmax = dt*length(h);
time = (0:dt:Tmax-dt);

S1=plot(time,PDP)
AX=gca;
set(AX,'FontSize',14);
T=title('Power Delay Profile');
set(T,'FontSize',14);
x=xlabel('Time [s]');
set(x,'FontSize',14);
y=ylabel('Power [V^2]');
set(y,'FontSize',14);

```

B. Evaluates the root mean square delay spread 'rmsds'

```

% Evaluates the root mean square dealy spread 'rmsds'
% of a channel impulse response 'h' sampled
% at frequency 'fc'
%
% Programmed by Guerino Giancola
%

function [rmsds,num1] = cp0802_rmsds(h,fc)

% -----
% Step One - Evaluation of the rms Delay Spread
% -----

dt = 1 / fc;          % sampling time

ns = length(h);      % number of samples representing
                    % the channel impulse response

time = (0 : dt : (ns-1)*dt);
den = sum(h.^2);
num1 = sum(time.*(h.^2)); % mean excess delay
num2 = sum((time.^2).*(h.^2));

% RMS spread delay-----
%law --: book- MIMO-OFDM Wireless Communications with MATLAB
% page- 16 . equ- 1.20
rmsds = sqrt((num2/den)-(num1/den)^2)
num1=(num1/den)

```

C. IEEE UWB Channel Model

```

%This function is almost unchanged from the original
cp0802_IEEEuwb.m
%programmed by Guerino Giancola. The author of the report has
added
%the parameter G as to prevent the graphic display.
%Parameters OT, ts, LAMBDA, lambda, Gamma and gamma have also been
%changed as to fit the LOS profile according to the proposals in
[2].
%Files cp0802_IEEEuwbLOS10.m, cp0802_IEEEuwbNLOS4.m, and
%cp0802_IEEEuwbNLOS10.m have been edited in the same way and will
%not be listed in the appendix.

```

```

%%%%%%%%%%%%%%%%%%%%%%%%%%%%%%%%%%%%%%%%%%%%%%%%%%%%%%%%%%%%%%%%%%%%%%%%
% FUNCTION 8.8 : "cp0802_IEEEuwb"
%
% Generates the channel impulse response for a multipath
% channel according to the statistical model proposed by
% the IEEE 802.15.SG3a.
%
% 'fc' is the sampling frequency
% 'TMG' is the total multipath gain
%
% The function returns:
% 1) the channel impulse response 'h0'
% 2) the equivalent discrete-time impulse response 'hf'
% 3) the value of the Observation Time 'OT'
% 4) the value of the resolution time 'ts'
% 5) the value of the total multipath gain 'X'
%
% Programmed by Guerino Giancola
%
function [h0,hf,OT,ts,X] = cp0802_IEEEuwbLOS10(fc, TMG, G);
% -----
% Step Zero - Input parameters
% -----
OT = 200e-9; % Observation Time [s]
ts = 1e-9; % time resolution [s]
%fc=22e9;
%fc=44e9;
% i.e. the 'bin' duration
LAMBDA = 0.015e9; % Cluster Arrival Rate (1/s)
lambda = 13e9; % Ray Arrival Rate (1/s)
GAMMA = 7.1e-9; % Cluster decay factor
    gamma = 4.3e-9; % Ray decay factor
sigma1 = 10^(3.3941/10); % Stdev of the cluster fading
sigma2 = 10^(3.3941/10); % Stdev of the ray fading
sigmax = 10^(3/10); % Stdev of lognormal shadowing
% ray decay threshold
rdt = 0.001;
% rays are neglected when exp(-t/gamma)<rdt
% peak treshold [dB]
PT = 50;
% rays are considered if their amplitude is
% within the -PT range with respect to the peak
% -----
% Step One - Cluster characterization

```

```

% -----
dt = 1 / fc; % sampling time
T = 1 / LAMBDA; % Average cluster inter-arrival time
% [s]
t = 1 / lambda; % Average ray inter-arrival time [s]
i = 1;
CAT(i)=0; % First Cluster Arrival Time
next = 0;
while next < OT
i = i + 1;
next = next + expinv(rand,T);
if next < OT
CAT(i)= next;
end
end % while remaining > 0
% -----
% Step Two - Path characterization
% -----
NC = length(CAT); % Number of observed clusters
logvar = (1/20)*((sigma1^2)+(sigma2^2))*log(10);
omega = 1;
pc = 0; % path-counter
for i = 1 : NC
pc = pc + 1;
CT = CAT(i); % cluster time
HT(pc) = CT;
next = 0;
mx = 10*log(omega)-(10*CT/GAMMA);
mu = (mx/log(10))-logvar;
a = 10^((mu+(sigma1*randn)+(sigma2*randn))/20);
HA(pc) = ((rand>0.5)*2-1).*a;
ccoeff = sigma1*randn; % fast fading on the cluster
while exp(-next/gamma)>rdt
pc = pc + 1;
next = next + expinv(rand,t);
HT(pc) = CT + next;
mx = 10*log(omega)-(10*CT/GAMMA)-(10*next/GAMMA);
mu = (mx/log(10))-logvar;
a = 10^((mu+ccoeff+(sigma2*randn))/20);
HA(pc) = ((rand>0.5)*2-1).*a;
end
end % for i = 1 : NC
% Weak peak filtering

```

```

peak = abs(max(HA));
limit = peak/10^(PT/10);
HA = HA .* (abs(HA)>(limit.*ones(1,length(HA))));
for i = 1 : pc
itk = floor(HT(i)/dt);
h(itk+1) = HA(i);
end
% -----
% Step Three - Discrete time impulse response
% -----
N = floor(ts/dt);
L = N*ceil(length(h)/N);
h0 = zeros(1,L);
hf = h0;
h0(1:length(h)) = h;
for i = 1 : (length(h0)/N)
tmp = 0;
for j = 1 : N
tmp = tmp + h0(j+(i-1)*N);
end
hf(1+(i-1)*N) = tmp;
end
% Energy normalization
E_tot=sum(h.^2);
h0 = h0 / sqrt(E_tot);
E_tot=sum(hf.^2);
hf = hf / sqrt(E_tot);
% Log-normal shadowing
mux = ((10*log(TMG))/log(10)) - (((sigmax^2)*log(10))/20);
X = 10^((mux+(sigmax*randn))/20);
h0 = X.*h0;
hf = X.*hf

%-----
% [rmsds]=cp0802_rmsds(h0,fc)
% [PDP]=cp0802_PDP(h0,fc)
%-----
% -----
% Step Four - Graphical Output
% -----
if G
Tmax = dt*length(h0);
time = (0:dt:Tmax-dt);
figure(1)

```

```
S1=stem(time,h0);
AX=gca;
set(AX,'FontSize',14);
T=title('Channel Impulse Response');
set(T,'FontSize',14);
x=xlabel('Time [s]');
set(x,'FontSize',14);
y=ylabel('Amplitude Gain');
set(y,'FontSize',14);
figure(2)
S2=stairs(time,hf);
AX=gca;
set(AX,'FontSize',14);
T=title('Discrete Time Impulse Response');
set(T,'FontSize',14);
x=xlabel('Time [s]');
set(x,'FontSize',14);
y=ylabel('Amplitude Gain');
set(y,'FontSize',14);
end
```

Indoor Localization with UWB and 2.4 GHz Bands

B. Barua, N. Kandil, N. Hakem, N. Zaarour

Laboratoire de recherche Télébec en communications souterraines (LRTCS)

Université du Québec en Abitibi-Témiscamingue (UQAT)

675, 1ère avenue, Val d'Or, QC, J9P 1Y3, QC, Canada.

Biki.Barua@uqat.ca, Nahi.Kandil@uqat.ca, nadir.hakem@uqat.ca, Nour.Zaarour@uqat.ca

Abstract— In this paper, we propose an approach based on time of arrival (TOA) using both ultra-wideband and IEEE 802.15.4 at 2.4 GHz technologies to achieve an enhanced localization accuracy. To this end, experimental TOA measurements have been performed for both technologies in an indoor university campus area with Obstructed LOS and NLOS propagation conditions. The experimental results pointed out different estimation of localization regarding the used technologies and propagation conditions. This difference is used to identify how to use both technologies in order to increase the accuracy of localization.

Keywords—Indoor localization, UWB, 2.4GHz, TOA

INTRODUCTION

Among all the applications in wireless sensor network (WSN), localization is one of the key aspect and most intensive research topic, particularly when a part of the network is mobile. In order to design a reliable localization scheme, several requirements and limitations have come out such as high accuracy, low cost design, low energy consumption, efficiency, etc. Although the global positioning system (GPS) is a wide known solution for localization and positioning in outdoor, it became irrelevant because of its high cost, lack of accuracy in indoor environment. Basically, localization methods are divided into two classes: ranging and range free techniques. Receiving signal strength indicator (RSSI), time of arrival (ToA), Time difference of arrival (TDoA) and angle of arrival [AoA] [1] are the most common signal proprieties used in ranging techniques; where number of hop in path between sensors, approximate point-in-triangulation test (APIT), centroid [2] are the most common network or network topology proprieties used in free range techniques. To support indoor localization techniques, various communication radio signal technologies were used to improve the accuracy and robustness. In [5], a localization algorithm has been proposed using RSSI for WSN using 2.4 GHz IEEE 802.15.4 communication technology. In [3], a positioning algorithm has been proposed based on a time of arrival on UWB communication technology for harsh environment. Even though each technology has different accuracy according to propagation conditions of the environment, the ranging propriety of signal and the signal itself, using more than one signal to support localization may increase the accuracy. So, in this paper, the TOA ranging algorithm is used to estimate the distance between sensors based on UWB and 2.4 GHz communication technology.

The idea behind using ToA based on UWB and 2.4 GHz communication technologies is to identify according to a

propagation conditions which technology gives high accuracy and propose an approach taken advantage of these technologies in order to enhance the localization processing.

METHODOLOGY

Time of Arrival (TOA)

Time of arrival (TOA) is a localization algorithm where the propagation delay between a well-known positioned nodes, so-called anchor, and unknown position nodes is used to estimate their positions. In TOA, synchronization between the nodes is required to improve the accuracy of localization. The mathematical representation is given below:

$$D_i = C * \tau = \sqrt{(x - x_i)^2 + (y - y_i)^2} \quad (1)$$

Where (x_i, y_i) represents the position of the anchor i and (x, y) represents the position of the unknown node. D_i is the estimated distance, C is the velocity of light, and τ is the time delay between the anchor i and the node with unknown location. In order to find the location of a node at least three equations involving three different anchors are needed. If the node is mobile more equations are needed.

Used Sensors

In our work, we used Nanotron solution to estimate distance from ToA for UWB and 2.4 GHz technology. Thus, we used Swarm bee ER module for UWB and Swarm bee LE module for 2.4 GHz. The operating band of swarm bee ER is 3.5 to 6.5 GHz, where the swarm bee LE module works between 2.4 and 2.4835 GHz ISM frequency band [4].

Measurement in Indoor environemnt

The indoor measurements were conducted, as illustrated fig. 1, in partly open intermediate floor in the building to the double-height ceilinged floor below at the university campus (UQAT). The wall is composed of wood and metal, where the floor is the concrete made. This area is divided in two sections: Line of sight (LOS) and Non line of sight (NLOS). But, in LOS area, 6 to 11 meters are introduced as obstructed line of sight (OLOS) for being surrounded by metallic cabinets, tables and glasses. Following the figure 2, NLOS measurement area is divided into two sections, where first 2 meters are define as LOS and the other 13 meters are define as NLOS. Clear vision of NLOS area is shown in both figure 1 and figure 2. The anchor sensors for both technologies have been placed at the height of 1 meters

from floor. Along with, for each technology we have used three anchor nodes and one unknown node that need to be localized. In total, 15 measurements have been carried out using directional UWB patch antenna and omnidirectional 2.4GHz antenna. In figure 2, measuring position for the LOS area is followed up by blue point and for NLOS area, starting point is denoted by the red point, then follow up the blue path of LOS till 13 meters.



Fig. 1. Measurement Environment.

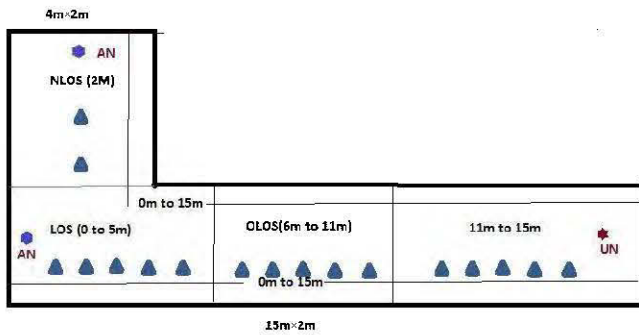


Fig. 2. Plan of measurement setup. AN (Anchor node) and UN (Unknown node) used to represent the presence of nodes in different environment.

RESULT AND ANALYSIS

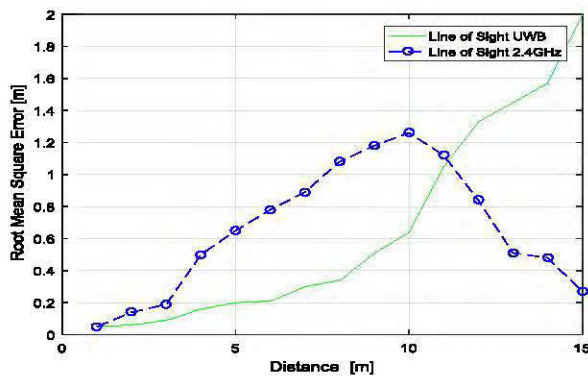


Fig. 3. Line of Sight Environment.

To analyze the result we calculate the root mean square error between actual distance and estimated distance. Figure 3 shows that root mean square error in LOS area is increasing gradually with the actual distance for both UWB and 2.4 GHz. After 10 m, the error for 2.4 GHz begin to decrease to reach less than 0.3m at 15 m actual distance. For UWB, the curve behavior continue to increase after 10 m. In figure 4, for the NLOS scenario the

error curve increase gradually with actual distance for both technologies and is higher comparatively to the LOS scenario. But at a distance around 10 meters, we can see an intersection point from where the level of error for 2.4 GHz comparatively lower than UWB. So, from our experiment it's shown that UWB technology perform better than 2.4GHz and the distance error is remarkably lower for 0 to 11 meters distance in LOS environment along with 0 to 10 meters for NLOS environment. On the other hand, for 2.4 GHz even though for the short range 0 to 11 meters for LOS and 0 to 10 meters for NLOS the rate of error is higher, beyond that this technology shows better performance than UWB. However, our work shows that UWB-TOA is more effective than 2.4GHz-TOA technique for short range in indoor environment.

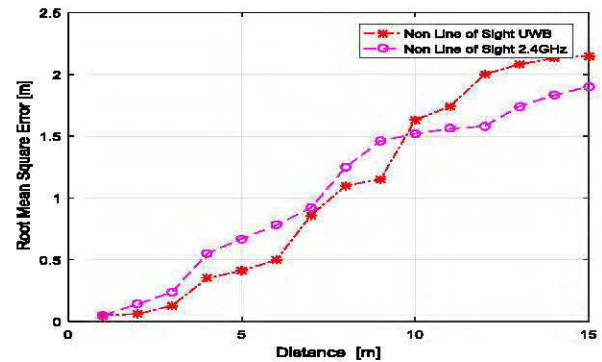


Fig. 4. Non line of sight (NLOS) Environment.

CONCLUSION

Our experimental work is aiming to propose the best technique for indoor localization as well as to establish a projectile threshold level for distance for both UWB and 2.4 GHz, in order to choose the best and efficient technology for localization. Experiment shows that for LOS in a range of 0 to 11, meters UWB is the best option and above that range 2.4 GHz is the best option. On the other hand, for NLOS in a range of 0 to 10 meters UWB is the best technology and beyond that range, 2.4 GHz is performing better for localization. In future work, this study will be applied to harsh environment such as mines.

References

- [1] Li, J., and Liu, H.-p.: 'A new weighted centroid localization algorithm in coal Mine wireless sensor networks', in Editor (Ed.) (Eds.): 'Book A new weighted centroid localization algorithm in coal Mine wireless sensor networks' (2011, edn.), pp. 106-109
- [2] Ahmad, T., Li, X.J., and Seet, B.C.: 'A self-calibrated centroid localization algorithm for indoor ZigBee WSNs', in Editor (Ed.) (Eds.): 'Book A self-calibrated centroid localization algorithm for indoor ZigBee WSNs' (2016, edn.), pp. 455-461
- [3] Chehri, A., Fortier, P., and Tardif, P.M.: 'UWB-based sensor networks for localization in mining environments', *Ad Hoc Networks*, 2009, 7, (5), pp. 987-1000
- [4] http://www.nanotron.com/EN/PR_find.php 1
- [5] Dincă, S., and Tudose, D.Ş.: 'Rssi-based localization in low-cost 2.4ghz wireless networks', in Editor (Ed.) (Eds.): 'Book Rssi-based localization in low-cost 2.4ghz wireless networks' (2013, edn.), pp. 1-5

FD-MIMO Relay Self-Interference Cancellation Using Space Projection Algorithms

Kazi Mustafizur Rahman, Nadir Hakem, Biki Barua
Telebec research laboratory for underground communications (LRTCS)
University of Quebec in Abitibi-Temiscamingue (UQAT)
675, 1st avenue, Val d'Or, QC, J9P 1Y3, QC, Canada.
kazimustafizur.rahman@uqat.ca, nadir.hakem@uqat.ca, Biki.barua@uqat.ca

Abstract— In this paper, self-interference (SI) cancellation algorithm based on Space Projection Algorithm (SPA) is proposed for Full-Duplex (FD) Multiple-Input Multiple-Output (MIMO) relays in an indoor wireless communication system. The simultaneous transmission and reception of the same radio signal imply a SI around the relay transceiver. The principal challenge of implementing the FD-MIMO relay is to this interference and increase the relaying capacity. To reach this aims, an efficient algorithm using SPA filters is designed and validated by simulation. The results of proposed method outperform the exiting works in term of BER for the QPSK modulation.

Keywords—FD relay; Self-Interference; Space Projection Algorithm; null space projection (NSP); subspace projection (SP); QPSK; MIMO.

I. INTRODUCTION

FD communication system has acquired much for its capability of simultaneously transmitting and receiving on the same signal at the same time [1]. The MIMO relay technology is a cost-effective approach since it can extend the coverage of the wireless system, provide higher spectral efficiency, improve network throughput by offering cooperative diversity and enhance the communication system capacity [2]. MIMO is the auspicious technology for the next-generation wireless communication system to provide a broad coverage area, incremented system capacity, and high spectral efficiency. The MIMO links are furnished with antenna arrays between both transmitter and receiver sides to maintain a high efficient multi-stream between the cessation-to-end antennas of the communication link [3] [4].

The relay approaches can be, also grouped into two broad categories, named as half-duplex (HD) and full-duplex (FD) relays. The FD methods are defined as a transceiver's ability to transmit and receive the same signal at the same time. Whereas, the HD relays require two orthogonal signals to achieve a single end-to-end link through a relay node. In the communication schemes, the FD relay is valuable in several anticipated features such as less delay, high efficiency, high security and improving access layer utility function [5]. Recently the FD relays are considered for infeasible inherent SI because FD enabled communication schemes are beneficial for many desired aspects. However, due to simultaneous transmission and reception, the self-interference (SI) caused by the coupling effect of the

transmitted signal at relay receiver become a rigorous issue in FD MIMO relay system. Consequently, the SI suppression in FD relay system is considered as an essential technique to ascertain the reliable transmission [6].

FD relays have been presented in an efficient short range application. According to the relay theory concept, SI signal is produced from the loopback (LI) signal. This signal has followed some signs such as high dynamic range of receiver or transmitter, faultless awareness of the SI path [7]. Hence the FD relay can receive the desired signals from the source end, while concurrently communicate the signals to the stage of destination. This ability gives the better results in decreasing the essential time slots on end-to-end communication and ignore the latency [8] [9].

The critical challenge to support FD relays is to resolve by suppression or cancellation SI induced by the loopback (LI) signal in the relay node. According to several works [10], [11], there are three main categories to suppress this SI: passive suppression (PS), analog cancellation (AC), and digital cancellation (DC). The majority of PS approaches rely on antenna design and placement to suppress the SI. They use intrinsic antenna parameters such as placement, directivity or polarization to keep isolation or space orthogonality around the relay to break the loop-back interference. The PS is better suited for a millimeter wave communication system where antenna separation is easy to achieve and may reach high SI suppression, for example, it may remove more than 40 dB interferences in 60 GHz band. In the AC approaches, the basic idea is to estimate and remove, at the analog RF stage, the SI signal received by the relay node. In [12], analog circuit domain cancellation technique purposes to mitigate the SI in the analog receive chain circuitry the DC. Unlike all the previous approaches, the DC approaches deferred SI processing to the digital RF level, in the form of digital SI canceler or receive beamforming. The digital SI canceler requires accurate estimation of residual SI to ensure that a small noise is introduced due errors estimation and signal distortion. Meanwhile, receive beamforming approaches are supported only by MIMO systems. In [13] presents the SI suppression strategies by FD-MIMO relay applying using antenna selection technique. They also discussed the conventional LI suppression scheme. Conventionally, LI could be suppressed by using zero forcing (ZF) and minimum mean square error (MMSE) estimation filter. Authors in [14] [15],

proposed null space projection and minimum mean square error filters for spatial loop interference suppression as well as discuss shortly how to combine them with time-domain cancellation. Despite all these approaches, complete cancellation of the SI signal has not been achieved to date.

In this paper, we proposed new algorithm stated to as the Two Stage Projection (TSPA) algorithm. TSPA consist of Null space projection (NSP) and Subspace Projection (SP) algorithm which can employ in the position when loopback (LI) channel matrix is of full rank. So, in this situation, we design receive and transmit filters combined with zero forcing (ZF) and also considered the multipath propagation of the LI signal. If the loop channel matrix is not of full rank, the NSP algorithm projected to cancel the loopback signal. SP algorithm primarily used to make the receive filter orthogonal to one subspace and the transmit filter orthogonal to another one to cancel the desired loop interference.

However, our paper is structured as follows: In section II, we introduce the system model of the two-hop relay. In section III, we present the proposed approach. Results and analysis has been introduced in section IV and the paper is concluded in section V.

II. SYSTEM MODEL

In this section, we provide a mathematical model of a relay station with SI occurrence and cancellation. A 3-node dual-hop amplifies and forward (AF) relaying system in the indoor wireless system is considered. AF relay always used for cooperative communication to improve the performance of the wireless system. AF relay amplifies its received signal and maintaining fixed average transmit power. In our system model, AF is employed because it requires relatively simple signal processing. The proposed technique considered for the two-hop relaying model.

The model includes Transmitter (T_x), Relay (R) and Receiver (R_x) nodes shown in Fig.1. The transmitter node is equipped with a set of N_{Tx} antennas whereas the receiver node has N_{Rx} antennas. The relay node is equipped with two sets of antennas. The first set, have N_R antennas and is dedicated to receiving meanwhile the second set include N_T transmit antennas.

We define $H_{TxR} \in \mathbb{C}^{N_R \times N_{Tx}}$ and $H_{RRx} \in \mathbb{C}^{N_{Rx} \times N_T}$ which represent the MIMO complex channel matrices respectively from the transmitter to relay node and from the relay node to a receiver. The signal vector $x(n)$ defined as a complex vector $x(n) \in \mathbb{C}^{N_{Tx} \times 1}$, transmitted by the source node. The complex signal vectors $r(n)$ and $t(n)$, stated as $r(n) \in \mathbb{C}^{N_R \times 1}$ and $t(n) \in \mathbb{C}^{N_T \times 1}$, denote respectively the received and transmitted signal at the relay node. H_{LI} is the SI signal, which

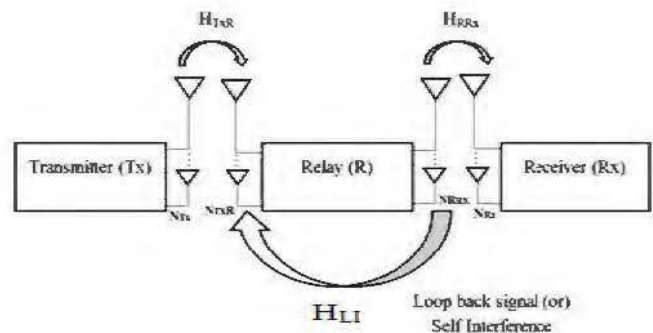


Fig. 5. Two-hop relay model.

reduces the channel capacity from the transmission to reception and makes the relay system unstable in FD-MIMO. The self-interference complex channel matrix, introduced by the relay, is denoted by $H_{LI} \in \mathbb{C}^{N_R \times N_T}$, as shown in fig. 1.

Time symbol (T_s) is the rate at which a signal is modulated, and it is a function of the symbol rate. i.e. for QPSK bit rate is $= \frac{2}{T_s}$. Since QPSK transmit two bit per symbol, and the symbol rate is $\frac{1}{T}$, QPSK can transmit 2 bits per second. The delay (d) is a measure of the multipath richness of a communications channel. In Fig.2. the signal power of each multipath is plotted against their respective propagation delays and it indicates how a transmitted pulse gets received at the receiver with different signal strength as it travels through a multipath channel with different propagation delays (τ_0, τ_1 and τ_2). The delay is mostly used in the characterization of wireless channels, but it also applies to any other multipath channel. According to the multipath delay of channel (d) and the time symbol of the signal (T_s), we can single out two cases. In both following situations, d will denote the maximum multi-path time delay of the channel.

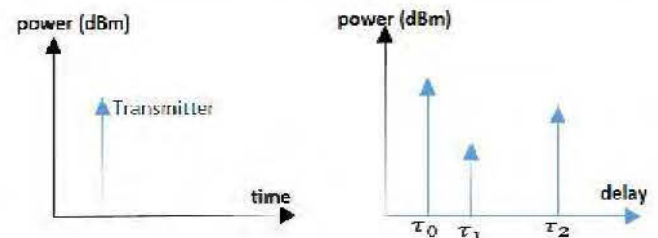


Fig. 6. Power delay profile (PDP).

A. First case ($d < T_s$)

In this case, the multipath parameter of the channel d is smaller than signal symbol time (T_s), which means that the one symbol will interfere mainly with itself. The signal received by the relay is expressed as,

$$r(n) = H_{TxR}x(n) + H_{LI}t(n) + w(n) \quad (1)$$

Where $w(n) \in \mathbb{C}^{N_R \times 1}$ denote an additive white Gaussian noise (AWGN) and $H_{LI}t(n)$ is the loopback interference signal received by the relay. Where $t(n)$ is the transmitted signal in the relay.

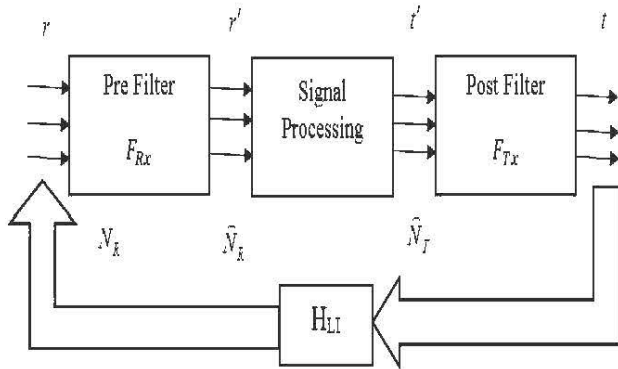


Fig. 7. Relay with loop back signal cancellation.

A pre-projection filter, which is called the LI signal suppression filter denoted by F_{Rx} and defined as $F_{Rx} \in \mathbb{C}^{N_R \times \hat{N}_R}$ and post-filter which is called transmit weight filter F_{Tx} defined by $F_{Tx} \in \mathbb{C}^{\hat{N}_T \times N_T}$ are depicted in fig.3. \hat{N}_R and \hat{N}_T are the received and transmit signal of the signal processor. Without loss of generality we can assume that $\hat{N}_R \leq N_R$ and $\hat{N}_T \leq N_T$ because the end to end communication cannot improve by the increasing the number of dimensions. The output signal of the pre- filter $r'(n) \in \mathbb{C}^{\hat{N}_R \times 1}$ and the input signal of the post filter $t'(n) \in \mathbb{C}^{N_T \times 1}$.

Now, the output of the pre-filter $r'(n)$ with loop back interference can be written as,

$$r'(n) = \{F_{Rx}(H_{TxR}x(n) + w(n))\} + \{F_{Rx}H_{LI}F_{Tx}t(n)\} \quad (2)$$

In equation 2, the first part represent the desired signal exposed to white Gaussian noise and the second part is channel loop back interference.

As shown in fig. 3, relay used two adaptive filters, pre filter F_{Rx} and post filter F_{Tx} to respectively process the input and output signal in order to cancel the SI. Which means that both filters will collaborate to define the right signal to send in order to suppress the channel loopback interference. To achieve this goal, according to equation 2, the second part should be zero (cf. equation 3) is a necessary and sufficient condition to optimize both adaptive filter weights.

$$F_{Rx}H_{LI}F_{Tx} = 0 \quad (3)$$

B. Second case ($d > T_s$)

For this case, the maximum multipath d induced by the channel LI is more than one time T_s duration. The number of subsequent symbols that interfere with one symbol, denoted by L , is estimated by equation 4.

$$L = \left\lceil \frac{d + \frac{T_s}{2}}{T_s} \right\rceil \quad (4)$$

The loop channel matrix $H_{LI} \in \mathbb{C}^{N_{Rx} \times (N_{Tx} \cdot L)}$ can be written as

$$H_{LI} = \begin{bmatrix} H_{11} & H_{12} & \dots & H_{1N_{Tx}} \\ H_{21} & H_{22} & \dots & H_{2N_{Tx}} \\ \vdots & \vdots & \ddots & \vdots \\ H_{N_{Rx}1} & H_{N_{Rx}2} & \dots & H_{N_{Rx}N_{Tx}} \end{bmatrix} \quad (5)$$

Where $H_{ij} \in \mathbb{C}^{1 \times L}$ is the sub channel vector from the i th transmit antenna to the j th receive antenna of the relay. Now, according to the model in fig.3 and due to the inter symbol interference the output signal $\hat{r}(n)$ is again presented as,

$$\hat{r}(n) = \{F_{Rx}(H_{TxR}x(n) + w(n))\} + \{F_{Rx}H_{LI}T(n)\} \quad (6)$$

Where $T(n) = [t_1(n) \ t_2(n) \ \dots \ t_{N_T}(n)]^T$ is an array of relay out coming signals, one per transmitting antenna and defined as:

$$t(n) = [t_i(n) \ t_i(n-1) \ \dots \ t_i(n-L+1)] \quad (7)$$

The $t_i(j)$ is the transmit signal by the i th relay antenna at sample time j . The output of the post filter relay node is,

$$t(n) = F_{Tx}t'(n) \quad (8)$$

Where $t'(n)$ indicated the input signal of the post filter.

$$\text{Let, } t'(n) = [t'_1(n), \ t'_2(n), \ \dots \ t'_{\hat{N}_T}(n)]$$

III. PROPOSED APPROACH

In this section, we showed the mathematical solution aspects of proposed algorithm. Substitute equation (8) in equation (6) we get,

$$r'(n) = \{F_{Rx}(H_{TxRx}(n) + w(n))\} + \{F_{Rx}H_{LI}\tilde{G}T(n)\} \quad (9)$$

Where $T'(n) = [\hat{t}_1(n) \ \hat{t}_2(n) \ \dots \ \hat{t}_{N_T}(n)]^T$ and \tilde{G} is the diagonal matrix of the adaptive filters.

P is the permutation matrix used to go to diagonalizable space.

$$\text{Where, } \tilde{G} = P^{-1} \text{diag}(F_{Tx}; L), \quad P = \begin{bmatrix} \text{diag}(Y_1; L) \\ \text{diag}(Y_2; L) \\ \vdots \\ \text{diag}(Y_L; L) \end{bmatrix}$$

$\text{diag}(Y, L)$ is the diagonal matrix with L diagonal components Y ; $\text{diag}(Y)$ is the diagonal matrix with diagonal components of each element of row vector Y .

In the case where is $L=1$, which mean that d is smaller than Ts , the F_{Rx} and F_{Tx} filters can be adapted using equation 3 as:

$$F_{Rx}H_{LI}P^{-1}\text{diag}(F_{Tx}; L) = 0 \quad (10)$$

When $L=1$, then equation (10) is rewritten as,

$$F_{Rx}[H_{L,1}, \ H_{L,2}, \ \dots \ H_{L,L}]\text{diag}(F_{Tx}; L) = 0 \quad (11)$$

$$\text{Where } H_{LI,k} = \begin{pmatrix} h_{11,k} & \dots & h_{1N_T,k} \\ \vdots & \ddots & \vdots \\ h_{NR,1,k} & \dots & h_{NR,N_T,k} \end{pmatrix}$$

Where $h_{ij,k}$ is the k th value of the row vector H_{ij} in equation (5). H_{LI} denoted by row space vector and H is denoted by column space vector. To achieve the sufficient condition of equation 10 is,

$$F_{Rx}H_{LI} = 0 \text{ and } [H_{L,1}^T, \ H_{L,2}^T, \ \dots \ H_{L,L}^T]^T F_{Tx} = 0 \quad (12)$$

Where, F_{Rx} is the pre space projection filter, F_{Rx} project the row space of H_{LI} to the null space of H_{LI} . Similar with F_{Tx} , F_{Tx} is the null space of $[H_{L,1}^T, \ H_{L,2}^T, \ \dots \ H_{L,L}^T]^T$.

A. *NSP with short rank loop interference matrix.*

The solution of (12), when the adaptive pre and post filters F_{Rx} and F_{Tx} , cannot be zero matrices, then.

$$0 < rf(H_{LI}) < N_R \text{ and } 0 < rf(H) < N_T \quad (13)$$

Where, the rank function rf gives the dimension of the vector space generated by matrix columns. The rank of a matrix would be zero only if the matrix had its elements equal to zero. If a matrix had even one non-zero element, its minimum rank would be one. $H = [H_{L,1}^T, \ H_{L,2}^T, \ \dots \ H_{L,L}^T]^T$. It means that only when the H_L or the H is not linearly independent matrix or not full rank the non-zero solution of equation (12) exist. With Zero Forcing algorithm, a solution of null space projection as,

$$F_{Rx} = I - H_{LI}H_{LI}^+ \quad (14)$$

$$F_{Tx} = I - HH^+ \quad (15)$$

Where $(.)^+$ is the Moore-Penrose pseudo-inverse and I is the identity matrix.

B. *Subspace Projection Partly Cancelling Interference (SSPCI) with Full Rank Matrix*

The second algorithm is called Subspace Projection Partly cancelling Interference (SPPCI). When the H_L and H are full rank, as

$$r(H_{LI}) = N_{Rx}; \ r(H) = N_{Tx} \quad (16)$$

We could just suppress the loop interference at the row space of H_{LI} or the column space of H . Choose the smaller positive integers C_1, C_2, D_1 and D_2 to satisfy both (17) and (18) equation.

$$r([H_{L,m_1}, \ H_{L,m_2}, \ \dots, \ H_{L,m_{D_1}}]) = N_R - C_1 \quad (17)$$

$$r([H_{L,n_1}^T, \ H_{L,n_2}^T, \ \dots, \ H_{L,n_{D_2}}^T]^T) = N_T - C_2 \quad (18)$$

Where $m_i, n_i \in [1, 2, \dots, L]$ we have the subspace

$$H_1 = [H_{L,m_1}, \ H_{L,m_2}, \ \dots, \ H_{L,m_{D_1}}] \quad (19)$$

$$H_2 = [H_{L,n_1}^T, \ H_{L,n_2}^T, \ \dots, \ H_{L,n_{D_2}}^T]^T \quad (20)$$

Then project the loop interference to the complementary space of H_1 or H_2 and the loop interference in space of H_1 or H_2 is cancelled by,

$$F_{Rx} = I - H_1 H_1^+ \quad (21)$$

$$F_{Tx} = I - H_2 H_2^+ \quad (22)$$

The nonlinearity of $f(\cdot)$ provide more degrees of choice to design the adaptive filters F_{Rx} and F_{Tx} . We can have two cases for relay transmitted signal. The Decode and Forward (DF) MIMO relay case, according to equation 23 where DF relay process the signal and regenerate source data streams, and the AF relay, according to equation 24, where the signal is forwarded after some basic processing.

The F_{Rx} and F_{Tx} have the equivalent function in AF relays, so they can be combined into one filter which would only mitigate the interference partly. The nonlinearity of $f(\cdot)$ provide more degrees of freedom for designing the F_{Rx} and F_{Tx} jointly, the loop interference suppression filter pairs are effective in the DF relays for completely suppressing the loop interference

$$t(n) = F_{Rx} f \left(F_{Rx}(r(n)) - w(n) \right) \quad (23)$$

$$t(n) = F_{Tx} F_{Rx}(r(n) + w(n)) \quad (24)$$

IV. RESULT AND DISCUSSION

The proposed model and TSPA approach are simulated with MATLAB software. The full-duplex MIMO relay is equipped with 6 antennas, three for each side ($N_R = N_T = 3$ antennas). The four phase QPSK modulation is considered. The loop back channel is independent Rayleigh fading channel because a close estimation of attenuation due to the multipath fading in wireless channels can be made by relay fading where the no line of sight component present and is normalized as $\|H_{LI}\| = N_R N_T$.

We evaluated the Bit Error Rate (BER) according to different Signal to Noise Ratio (SNR) for both condition, i.e., when the delay is less than the time symbol and delay is greater than time symbol. The relation between the SI, BER and SNR is

$$SNR = \frac{S}{N}; N = W_n + SI$$

Where N is the noise, W_n is the white noise and SI is the self-interference.

Fig.4. shows that the BER of the relay is a function of the signal-to-noise ratio (SNR). The simulation shows that even the rank of loop interference matrix is full, it's possible to eliminate the loop interference entirely by jointly design receive and transmit space projection filter.

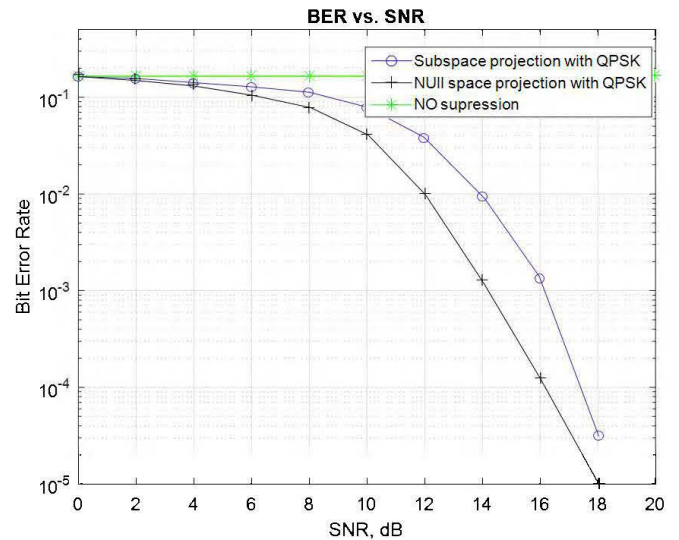


Fig.4. Bit Error Rate VS Signal to Noise Ratio, when $(d < T_s)$

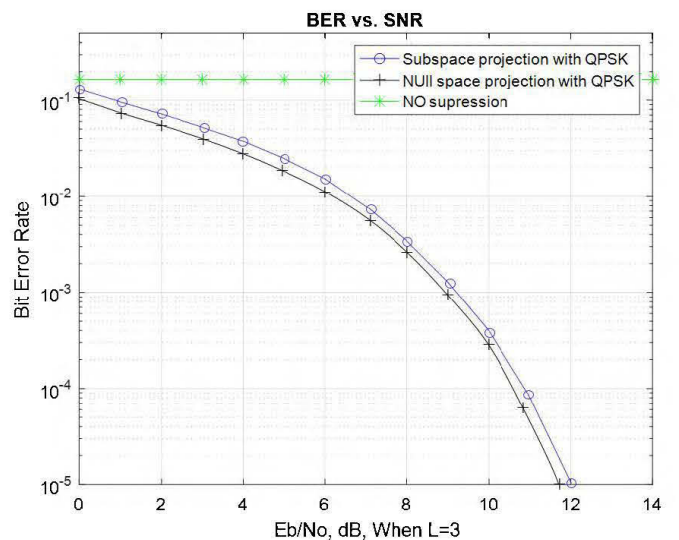


Fig.5. Bit Error Rate VS Signal to Noise Ratio

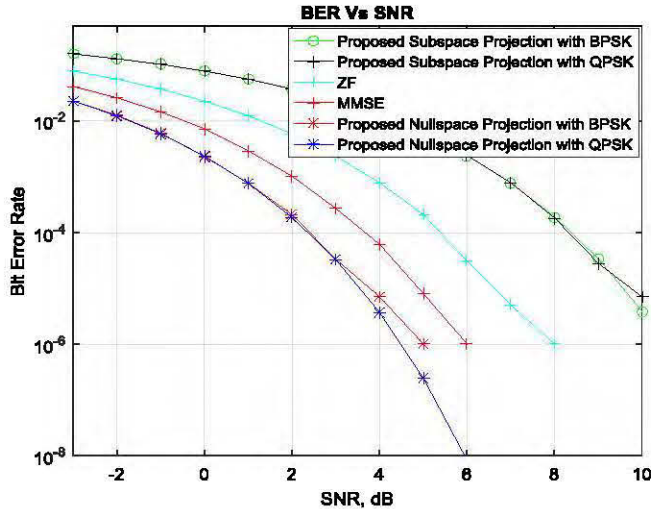


Fig.6. Bit Error Rate VS Signal to Noise Ratio Compare to ZF, MMSE and Proposed Scheme

Fig.5. shows that the BER of the relay is a function of the signal-to-noise ratio (SNR). The simulation shows that even when the delay is greater than the one-time symbol, it is possible to eliminate the most of the loop back interference by cooperatively design receive and transmit space projection filter. The Null space projection (SPA) can entirely mitigate the known and partly unknown component of the self-interference and the subspace projection filter where's the Subspace projection (SP) reduce the known part when the number L is three time the T_s duration.

Fig. 6 compared the BER performance of the Zero forcing (ZF), Minimum Mean Square Error (MMSE) and proposed two stage projection with BPSK and QPSK modulation. The simulation shows that the BER performance of MMSE and ZF gives performance than proposed subspace algorithm with BPSK and QPSK. However, Proposed Two Stage Projection (TSPA) with four phase QPSK gives better BER Performance than MMSE, ZF and proposed two stage algorithm with BPSK. From the comparison, we can see that our proposed scheme (TSPA) with QPSK can mitigate the self-interference more than 70% than other existing conventional LI suppression method.

V. CONCLUSION

This article develops the FD-MIMO relays SI cancellation model for the indoor wireless communication systems. The significant self-interface cancellation is achieved by using SPA with QPSK modulation, where SPA consists of two space projection filters. In multipath channel, simulation results give better and significant cancellation of SI for QPSK modulation and outperform existing works. The first space projection filter reduces effectively the BER where the second one bring a significant enhancement, at least by 60%, in multipath propagation channel conditions. In the next step of this work is we to perform this operation for harsh environment such as underground mine.

References

- [6] Xin Quan, Ying Liu, Wensheng Pan, "A two-stage analog cancellation architecture for self-interference suppression in full-duplex communications," 2017 *IEEE MTT-S International Microwave Symposium (IMS)*, Y1 - 4-9 June 2017.
- [7] R. Askar, T. Kaiser, B. Schubert, T. Haustein, and W. Keusgen, "Active self-interference cancellation mechanism for full-duplex wireless transceivers," in 2014 9th International Conference on Cognitive Radio Oriented Wireless Networks and Communications (CROWNCOM), pp. 539-544, 2014.
- [8] Ahmed Almradi, "On the Performance of MIMO Full-Duplex Relaying in the Presence of Co-Channel Interference," Global Communications Conference (GLOBECOM), December 2016.
- [9] Ahmed Almradi, Khairi Ashour Hamdi, "MIMO Full-Duplex Relaying in the Presence of Co-Channel Interference," *IEEE Transactions on Vehicular Technology*, vol. 66, June 2017.
- [10] A.-R. Emilio, W. Stefan, R. López-Valcarce, R. Taneli, and W. Risto, "Wideband Full-Duplex MIMO Relays with Blind Adaptive Self-Interference Cancellation," *Signal Processing*, vol. 130, 2017.
- [11] Yi Yang, Yanhua Sun, Enchang Sun, "Evidence Theory Based Self-Interference Suppression for Two-Way Full-Duplex MIMO Relays," International Conference on *Computer and Information Technology; Ubiquitous Computing and Communications; Dependable, Autonomic and Secure Computing; Pervasive Intelligence and Computing (CIT/IUCC/DASC/PICOM)*, oct. 2015.
- [12] N. Bornhorst and M. Pesavento, "Filter-and-forward beamforming with adaptive decoding delays in asynchronous multi-user relay networks," *Signal Process.*, vol. 109, pp. 132-147, 2015.
- [13] S. Huberman and T. Le-Ngoc, "Self-Interference-Threshold-Based MIMO Full-Duplex Precoding," *IEEE Transactions on Vehicular Technology*, vol. 64, pp. 3803-3807, 2015.
- [14] M. Sakai, H. Lin, and K. Yamashita, "Self-interference cancellation in full-duplex wireless with IQ imbalance," *Physical Communication*, vol. 18, Part 1, pp. 2-14, 3// 2016.
- [15] P. Mathecken, T. Riihonen, S. Werner, and R. Wichman, "Constrained Phase Noise Estimation in OFDM Using Scattered Pilots Without Decision Feedback," *IEEE Transactions on Signal Processing*, vol. 65, pp. 2348-2362, 2017.
- [16] Z. Wei, X. Zhu, S. Sun, Y. Huang, L. Dong, and Y. Jiang, "Full-Duplex Versus Half-Duplex Amplify-and-Forward Relaying: Which is More Energy Efficient in 60-GHz Dual-Hop Indoor Wireless Systems?," *IEEE Journal on Selected Areas in Communications*, vol. 33, pp. 2936-2947, 2015.
- [17] D. Liang, P. Xiao, G. Chen, M. Ghorashi, and R. Tafazolli, "Digital self-interference cancellation for Full-Duplex MIMO systems," in 2015 *International Wireless Communications and Mobile Computing Conference (IWCMC)*, pp. 403-407, 2015.
- [18] Y. Sung, J. Ahn, B. Van Nguyen, and K. Kim, "Loop-interference suppression strategies using antenna selection in full-duplex MIMO relays," in *Intelligent Signal Processing and Communications Systems (ISPACS), 2011 International Symposium on*, pp. 1-4, 2011.
- [19] T. Riihonen, S. Werner, and R. Wichman, "Spatial loop interference suppression in full-duplex MIMO relays," in 2009 *Conference Record of the Forty-Third Asilomar Conference on Signals, Systems and Computers*, pp. 1508-1512, 2009.
- [20] T. Riihonen, S. Werner and R. Wichman, "Mitigation of loopback selfinterference in full-duplex MIMO relays," *IEEE Trans. Signal Process.*, vol. 59, no. 12, pp. 5983-5993, Dec. 2011.

Self-Interference Mitigation in Two-Hop Relay Using Two Stage Projection Algorithms

Kazi Mustafizur Rahman, Nadir Hakem, Biki Barua

Telebec research laboratory for underground communications (LRTCS)

University of Quebec in Abitibi-Temiscamingue (UQAT)

675, 1st avenue, Val d'Or, QC, J9P 1Y3, QC, Canada.

kazimustafizur.rahman@uqat.ca, nadir.hakem@uqat.ca, Biki.barua@uqat.ca

Abstract— This paper develops an efficient Self-Interference (SI) mitigation algorithm for Multiple-Input and Multiple-Output (MIMO) for Full-Duplex (FD) relays in the indoor wireless communication system. The relayed signal create an SI around the relay transceivers due to the loop-back (LI) signals. The main challenge of implementing FD-MIMO relay is to mitigate the performance degradation induced by the SI. This paper presents an efficient algorithm using Two Stage Projection Algorithm (TSPA) to reduce or remove the SI. The simulation results show that the proposed method minimize efficiently the SI.

Keywords—Dual-hop relays; Self-Interference; two Stage Projection Algorithm (TSPA); null space projection (NSP); subspace projection (SP); MIMO.

VI. INTRODUCTION

Relaying is a promising technique to provide lower transmit powers, higher throughput and enhance the coverage in the future wireless communication system. The FD-MIMO relay provides a promising approach to wireless communication systems, and it can improve 3GPP association in the technical specification of 5G mobile wireless communication system [1]. MIMO relay technology is a cost-effective approach since it can extend the coverage of the wireless system, provide higher spectral efficiency, improve network throughput by offering cooperative diversity and enhance the communication system capacity [2] [3].

Nowadays, MIMO is the favorable technology for next generation wireless communication system to provide a wide coverage area, increased system capacity and high spectral efficiency. The MIMO links are furnished with antenna arrays between both transmitter and receiver sides to maintain a high

efficient multi-stream between the end-to-end antennas of the communication link [4].

The relay approaches can be, also grouped into two broad categories, named as half-duplex (HD) and full-duplex (FD) relays. The FD methods are defined as a transceiver's ability to transmit and receive the same signal at the same time. Whereas, the HD relays require two orthogonal signals to achieve a single end-to-end link through a relay node. In the communication schemes, the FD relay is valuable in several anticipated features such as less delay, high efficiency, high security and improving access layer utility function [5]. Recently the FD relays are considered for infeasible inherent SI because FD enabled communication schemes are beneficial for many desired aspects (i.e., lower delay and higher efficiency, etc.). Thereby the exploiting specialized mitigation techniques were added in FD communications [6].

FD relays have been presented in an efficient short range application. According to the relay theory concept, SI signal is produced from the loopback (LI) signal. This signal has followed some signs such as high dynamic range of receiver or transmitter, faultless awareness of the SI path [7]. Hence the FD relay can receive the desired signals from the source end; while concurrently communicate the signals to the stage of destination. This ability gives the better results in decreasing the essential time slots on end-to-end communication and ignore the latency [8] [9].

The critical challenge to support FD relays is to resolve by suppression or cancellation SI induced by the LI signal in the relay node. According to several works [10], [11], there are three main categories to suppress this SI: passive suppression (PS), analog cancellation (AC), and digital cancellation (DC). The majority of PS approaches rely on antenna design and placement to suppress the SI. They use intrinsic antenna parameters such as placement, directivity or polarization to keep isolation or space orthogonality around the relay to break the loop-back interference. The PS is better suited for a millimeter wave communication system where antenna separation is easy to achieve and may reach high SI suppression, for example, it may remove more than 40 dB interferences in 60 GHz band. In

the AC approaches, the basic idea is to estimate and remove, at the analog RF stage, the SI signal received by the relay node. In [12], analog circuit domain cancellation technique purposes to mitigate the SI in the analog receive chain circuitry the DC. Unlike all the previous approaches, the DC approaches deferred SI processing to the digital RF level, in the form of digital SI canceler or receive beamforming. The digital SI canceler requires accurate estimation of residual SI to ensure that a small noise is introduced due errors estimation and signal distortion. Meanwhile, receive beamforming approaches are supported only by MIMO systems. In [13] presents the SI suppression strategies by FD-MIMO relay applying using antenna selection technique. They also discussed the conventional LI suppression scheme. Conventionally, LI could be suppressed by using ZF and MMSE estimation filter. Authors in [14] proposed null space projection and minimum mean square error filters for spatial loop interference suppression as well as discuss shortly how to combine them with time-domain cancellation. Despite all these approaches, complete mitigation of the SI signal has not been achieved to date.

In this paper, we proposed new algorithm stated to as the Two Stage Projection (TSPA) algorithm. TSPA consist of Null space projection (NSP) and Subspace Projection (SP) algorithm which can employ in the position when loop back (LI) channel matrix is of full rank. So, in this situation, we design a receive and transmit filters combined with zero forcing (ZF) and also considered the multipath propagation of the LI signal. If the loop channel matrix is not of full rank, the NSP algorithm projected to cancel the loop back signal. SP algorithm primarily used to make the receive filter orthogonal to one subspace and the transmit filter orthogonal to another one to cancel the desired loop interference.

The paper is structured as follows: In section II, we introduce the system model of the two-hop relay. In section III, we present the proposed approach. Results and analysis has been introduced in section IV and the paper is concluded in section V.

VII. SYSTEM MODEL

In this section, we provide a mathematical model of a relay station with SI occurrence and mitigation. A 3-node dual-hop amplifies and forward (AF) relaying system in the indoor wireless system is considered AF relay always used for cooperative communication to improve the performance of the wireless system AF relay amplifies its received signal and maintaining fixed average transmit power. In our system model, AF is employed because it requires relatively simple signal processing. The proposed technique considered for the two-hop relaying model.

The model includes Transmitter (T_x), Relay (R) and Receiver (R_x) nodes shown in Fig.1. The transmitter node is equipped with a set of N_{Tx} antennas whereas the receiver node has N_{Rx} antennas. The relay node is equipped with two sets of antennas. The first set, have N_R antennas and is dedicated to receiving meanwhile the second set include N_T transmit antennas.

We define $H_{TxR} \in \mathbb{C}^{N_R \times N_{Tx}}$ and $H_{RRx} \in \mathbb{C}^{N_{Rx} \times N_T}$ which represent the MIMO complex channel matrices respectively

from the transmitter to relay node and from the relay node to a receiver. The signal vector $x(n)$ defined as a complex vector $x(n) \in \mathbb{C}^{N_{Tx} \times 1}$, transmitted by the source node. The complex signal vectors $r(n)$ and $t(n)$, stated as $r(n) \in \mathbb{C}^{N_R \times 1}$ and $t(n) \in \mathbb{C}^{N_T \times 1}$, denote respectively the received and transmitted signal at the relay node. H_{LI} is the SI signal which

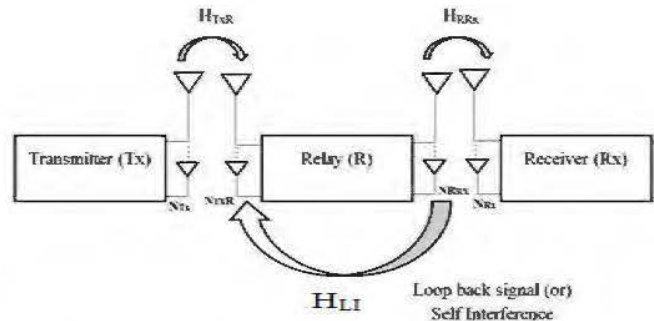


Fig. 8. Two-hop relay model.

reduces the channel capacity from the transmission to reception and makes the relay system unstable in FD-MIMO. The self-interference complex channel matrix, introduced by the relay, is denoted by $H_{LI} \in \mathbb{C}^{N_R \times N_T}$, as shown in fig. 1.

Time symbol (T_s) is the rate at which a signal is modulated, and it is a function of the symbol rate. i.e. for BPSK bit rate is equal to symbol rate (T_s). Since BPSK transmit one bit per symbol, and the symbol rate is $\frac{1}{T}$, BPSK can transmit $\frac{1}{T}$ bits per second. The delay (d) is a measure of the multipath richness of a communications channel. In Fig.2, the signal power of each multipath is plotted against their respective propagation delays and it indicates how a transmitted pulse gets received at the receiver with different signal strength as it travels through a multipath channel with different propagation delays (τ_0, τ_1 and τ_2). The delay is mostly used in the characterization of wireless channels, but it also applies to any other multipath channel. According to the multipath delay of channel (d) and the time symbol of the signal (T_s), we can single out two cases. In both following situations, d will denote the maximum multipath time delay of the channel.

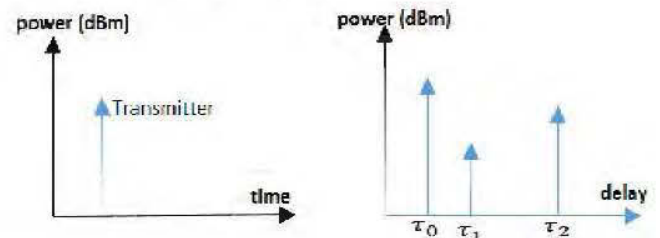


Fig. 9. Power delay profile.

A. First case ($d < T_s$)

In this case, the multipath parameter of the channel d is smaller than signal symbol time (T_s), which means that the one

symbol will interfere mainly with itself. The signal received by the relay is expressed as,

$$r(n) = H_{TxR}x(n) + H_{Li}t(n) + w(n) \quad (1)$$

Where $w(n) \in \mathbb{C}^{N_R \times 1}$ denote an additive white Gaussian noise (AWGN) and $H_{Li}t(n)$ is the loopback interference signal received by the relay. Where $t(n)$ is the transmitted signal in the relay.

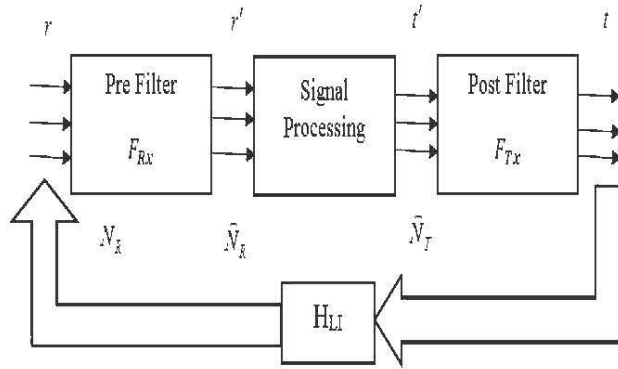


Fig. 10. Relay with loop back signal cancellation.

A pre-projection filter, which is called the LI signal suppression filter denoted by F_{Rx} and defined as $F_{Rx} \in \mathbb{C}^{N_R \times \tilde{N}_R}$ and post-filter which is called transmit weight filter F_{Tx} defined by $F_{Tx} \in \mathbb{C}^{\tilde{N}_T \times N_T}$ are depicted in fig.3. \tilde{N}_R and \tilde{N}_T are the received and transmit signal of the signal processor. Without loss of generality we can assume that $\tilde{N}_R \leq N_R$ and $\tilde{N}_T \leq N_T$ because the end to end communication cannot improve by the increasing the number of dimensions. The output signal of the pre- filter $r'(n) \in \mathbb{C}^{\tilde{N}_R \times 1}$ and the input signal of the post filter $t'(n) \in \mathbb{C}^{N_T \times 1}$.

Now, the output of the pre-filter $r'(n)$ with loop back interference can be written as,

$$r'(n) = \{F_{Rx}(H_{TxR}x(n) + w(n))\} + \{F_{Rx}H_{Li}F_{Tx}t(n)\} \quad (2)$$

In equation 2, the first part represent the desired signal exposed to white Gaussian noise and the second part is channel loop back interference.

As shown in fig. 3, relay used two adaptive filters, pre filter F_{Rx} and post filter F_{Tx} to respectively process the input and output signal in order to cancel the SI. Which means that both filters will collaborate to define the right signal to send in order to suppress the channel loopback interference. To achieve this goal, according to equation 2, the second part should be zero (cf. equation 3) is a necessary and sufficient condition to optimize both adaptive filter weights.

$$F_{Rx}H_{Li}F_{Tx} = 0 \quad (3)$$

B. Second case ($d > T_s$)

For this case, the maximum multipath d induced by the channel LI is more than one time T_s duration. The number of subsequent symbols that interfere with one symbol, denoted by L , is estimated by equation 4.

$$L = \left\lceil \frac{d + \frac{T_s}{2}}{T_s} \right\rceil \quad (4)$$

The loop channel matrix $H_{Li} \in \mathbb{C}^{N_{Rx} \times (N_{Tx} \cdot L)}$ can be written as

$$H_{Li} = \begin{bmatrix} H_{11} & H_{12} \cdots & H_{1N_{Tx}} \\ H_{21} & H_{22} \cdots & H_{2N_{Tx}} \\ \vdots & \vdots & \vdots \\ H_{N_{Rx}1} & H_{N_{Rx}2} & H_{N_{Rx}N_{Tx}} \end{bmatrix} \quad (5)$$

(5)

Where $H_{ij} \in \mathbb{C}^{1 \times L}$ is the sub channel vector from the i th transmit antenna to the j th receive antenna of the relay. Now, according to the model in fig.3 and due to the inter symbol interference the output signal $\hat{r}(n)$ is again presented as,

$$\hat{r}(n) = \{F_{Rx}(H_{TxR}x(n) + w(n))\} + \{F_{Rx}H_{Li}T(n)\} \quad (6)$$

Where $T(n) = [t_1(n) \ t_2(n) \ \dots \ t_{N_T}(n)]^T$ is an array of relay out coming signals, one per transmitting antenna and defined as:

$$t(n) = [t_i(n) \ t_i(n-1) \ \dots \ t_i(n-L+1)] \quad (7)$$

The $t_i(j)$ is the transmit signal by the i th relay antenna at sample time j . The output of the post filter relay node is,

$$t(n) = F_{Tx}t'(n) \quad (8)$$

Where $t'(n)$ indicated the input signal of the post filter.

$$\text{Let, } t'(n) = [t'_1(n), \ t'_2(n), \ \dots \ t'_{\tilde{N}_T}(n)]$$

VIII. PROPOSED APPROACH

In this section, we showed the mathematical solution aspects of proposed algorithm. Substitute equation (8) in equation (6) we get,

$$r'(n) = \{F_{Rx}(H_{TxR}x(n) + w(n))\} + \{F_{Rx}H_{LI}\tilde{G}T(n)\} \quad (9)$$

Where $T'(n) = [t_1(n) \ t_2(n) \ \dots \ t_{\hat{N}_T}(n)]^T$ and \tilde{G} is the diagonal matrix of the adaptive filters.

P is the permutation matrix used to go to diagonalizable space.

$$\text{Where, } \tilde{G} = P^{-1} \text{diag}(F_{Tx}; L), \quad P = \begin{bmatrix} \text{diag}(Y_1; L) \\ \text{diag}(Y_2; L) \\ \vdots \\ \text{diag}(Y_L; L) \end{bmatrix}$$

$\text{Diag}(Y, L)$ is the diagonal matrix with L diagonal components Y ; $\text{diag}(Y)$ is the diagonal matrix with diagonal components of each element of row vector Y .

In the case where is $L=1$, which mean that d is smaller than Ts , the F_{Rx} and F_{Tx} filters can be adapted using equation 3 as:

$$F_{Rx}H_{LI}P^{-1}\text{diag}(F_{Tx}; L) = 0 \quad (10)$$

When $L=1$, then equation (10) is rewritten as,

$$F_{Rx}[H_{L,1}, \ H_{L,2}, \ \dots \ H_{L,L}]\text{diag}(F_{Tx}; L) = 0 \quad (11)$$

$$\text{Where } H_{LI,K} = \begin{pmatrix} h_{11,k} & \dots & h_{1N_T,k} \\ \vdots & \ddots & \vdots \\ h_{NR1,k} & \dots & h_{NRN_T,k} \end{pmatrix}$$

Where $h_{ij,k}$ is the k th value of the row vector H_{ij} in equation (5). H_{LI} denoted by row space vector and H is denoted by column space vector. To achieve the sufficient condition of equation 10 is,

$$\begin{aligned} F_{Rx}H_{LI} &= 0 \text{ and} \\ [H_{L,1}^T, \ H_{L,2}^T, \ \dots \ H_{L,L}^T]^T F_{Tx} &= 0 \end{aligned} \quad (12)$$

Where, F_{Rx} is the pre space projection filter, F_{Rx} project the row space of H_{LI} to the null space of H_{LI} .

Similar with F_{Tx} , F_{Tx} is the null space of $[H_{L,1}^T, \ H_{L,2}^T, \ \dots \ H_{L,L}^T]^T$.

A. NSP with short rank loop interference matrix.

The solution of (12), when the adaptive pre and post filters F_{Rx} and F_{Tx} , cannot be zero matrices, then.

$$0 < rf(H_{LI}) < N_R \text{ and } 0 < rf(H) < N_T \quad (13)$$

Where, the rank function rf gives the dimension of the vector space generated by matrix columns. The rank of a matrix would be zero only if the matrix had its elements equal to zero. If a matrix had even one non-zero element, its minimum rank would be one. $H = [H_{L,1}^T, \ H_{L,2}^T, \ \dots \ H_{L,L}^T]^T$. It means that only when the H_L or the H is not linearly independent matrix or not full rank the non-zero solution of equation (12) exist. With Zero Forcing algorithm, a solution of null space projection as,

$$F_{Rx} = I - H_{LI}H_{LI}^+ \quad (14)$$

$$F_{Tx} = I - HH^+ \quad (15)$$

Where $(.)^+$ is the Moore-Penrose pseudo-inverse and I is the identity matrix.

B. Subspace Projection Partly Cancelling Interference (SSPCI) with Full Rank Matrix

The second algorithm is called Subspace Projection Partly cancelling Interference (SPPCI). When the H_L and H are full rank, as

$$r(H_{LI}) = N_{Rx}; \ r(H) = N_{Tx} \quad (16)$$

We could just suppress the loop interference at the row space of H_{LI} or the column space of H . Choose the smaller positive integers C_1, C_2, D_1 and D_2 to satisfy both (17) and (18) equation.

$$r([H_{L,m_1}, \ H_{L,m_2}, \ \dots, \ H_{L,m_{D_1}}]) = N_R - C_1 \quad (17)$$

$$r([H_{L,n_1}^T, \ H_{L,n_2}^T, \ \dots, \ H_{L,n_{D_2}}^T]^T) = N_T - C_2 \quad (18)$$

Where $m_i, n_i \in [1, 2, \dots, L]$ we have the subspace

$$H_1 = [H_{L,m_1}, H_{L,m_2}, \dots, H_{L,m_{D_1}}] \quad (19)$$

$$H_2 = [H_{L,n_1}^T, H_{L,n_2}^T, \dots, H_{L,n_{D_2}}^T]^T \quad (20)$$

Then project the loop interference to the complementary space of H_1 or H_2 and the loop interference in space of H_1 or H_2 is cancelled by,

$$F_{Rx} = I - H_1 H_1^+ \quad (21)$$

$$F_{Tx} = I - H_2 H_2^+ \quad (22)$$

The nonlinearity of $f(\cdot)$ provide more degrees of choice to design the adaptive filters F_{Rx} and F_{Tx} . We can have two cases for relay transmitted signal. The Decode and Forward (DF) MIMO relay case, according to equation 23 where DF relay process the signal and regenerate source data streams, and the AF relay, according to equation 24, where the signal is forwarded after some basic processing.

The F_{Rx} and F_{Tx} have the equivalent function in AF relays, so they can be combined into one filter which would only mitigate the interference partly. The nonlinearity of $f(\cdot)$ provide more degrees of freedom for designing the F_{Rx} and F_{Tx} jointly, the loop interference suppression filter pairs are effective in the DF relays for completely suppressing the loop interference

$$t(n) = F_{Rx} f(F_{Rx}(r(n)) - w(n)) \quad (23)$$

$$t(n) = F_{Tx} F_{Rx}(r(n) + w(n)) \quad (24)$$

IX. RESULT AND DISCUSSION

The proposed model and TSPA approach are simulated with MATLAB software. The full-duplex MIMO relay is equipped with 6 antennas, three for each side ($N_R = N_T = 3$ antennas). The BPSK modulation is considered. The loop back channel is independent Rayleigh fading channel because a close estimation of attenuation due to the multipath fading in wireless channels can be made by relay fading where the no line of sight component present and is normalized as $\|H_{Ll}\| = N_R N_T$

We evaluated the Bit Error Rate (BER) according to different Signal to Noise Ratio (SNR) for both condition, i.e., when the delay is less than the time symbol and delay is greater than time symbol. The relation between the SI, BER and SNR is

$$SNR = \frac{S}{N}; N = W_n + SI$$

Where N is the noise, W_n is the white noise and SI is the self-interference.

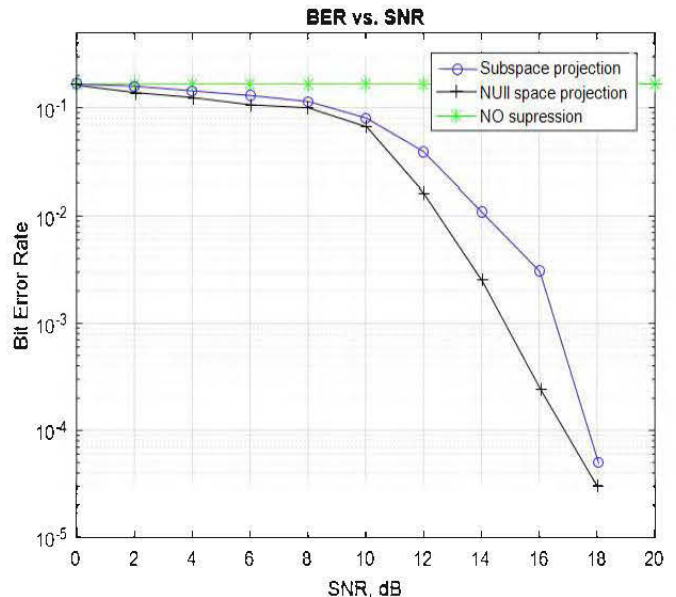


Fig.4. Bit Error Rate VS Signal to Noise Ratio, when $(d < T_s)$

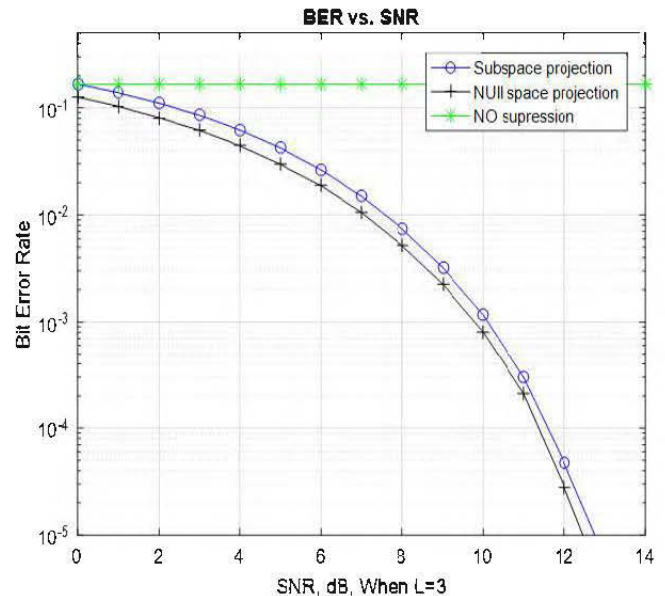


Fig.5. Bit Error Rate VS Signal to Noise Ratio, when $L=3$

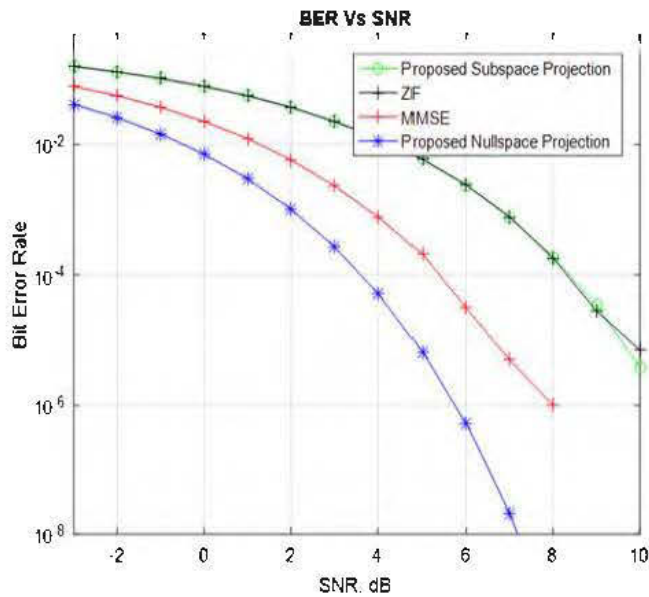


Fig. 6. Bit Error Rate VS Signal to Noise Ratio Compare to ZF, MMSE and Proposed Scheme

Fig. 4. shows that the BER of the relay is a function of the signal-to-noise ratio (SNR). The simulation shows that even the rank of loop interference matrix is full, it's possible to eliminate the loop interference entirely by jointly design a receive and transmit space projection filter.

Fig. 5. Shows that the BER of the relay is a function of the signal-to-noise ratio (SNR). The simulation shows that even when the delay is greater than the one time symbol, it is possible to eliminate the most of the loop back interference by cooperatively design receive and transmit space projection filter. The Null space projection (NSP) can entirely mitigate the known and partly unknown component of the self-interference and the subspace projection filter where's the Subspace projection (SP) reduce the known part when the number L is three time the T_s duration.

Fig. 6 compared the BER performance of the Zero forcing (ZF), Minimum Mean Square Error (MMSE) and proposed two stage projection. The simulation shows that the BER curve of MMSE, in red color, is better than ZF and proposed subspace projection. However, Proposed Two Stage Projection (TSPA) gives better BER Performance than MMSE and ZF. From the comparison, we can see that our proposed scheme (TSPA) can mitigate the self-interference 70% more than other existing conventional loop back suppression method.

X. CONCLUSION

This paper proposed an efficient Self-Interference cancellation algorithm for FD-MIMO relays in indoor wireless systems. Our primary concern was to mitigate the relay SI. The SI mitigation is achieved by using TSPA. It consists of two stages called NSP and SP. We observed the simulation for two conditions related to the symbol time duration and the maximum delay of the multipath channel where the relay is deployed. As

preliminary results, two space projection scheme gives better and significant cancellation of SI. Subspace projection has better system stability, and it may cancel the loop back by reducing the BER significantly. The second stage null space project support and increase this enhancement at least by 50% for multipath and one path propagation channel. As future work, the number of relay antenna changing effect in harsh environments will be considered.

References

- [21] O. Taghizadeh, J. Zhang, and M. Haardt, "Transmit beamforming aided amplify-and-forward MIMO full-duplex relaying with limited dynamic range," *Signal Process.*, vol. 127, pp. 266-281, 2016.
- [22] R. Askar, T. Kaiser, B. Schubert, T. Haustein, and W. Keusgen, "Active self-interference cancellation mechanism for full-duplex wireless transceivers," in *2014 9th International Conference on Cognitive Radio Oriented Wireless Networks and Communications (CROWNCOM)*, pp. 539-544, 2014.
- [23] A. Tang and X. Wang, "Balanced RF-circuit based self-interference cancellation for full duplex communications," *Ad Hoc Netw.*, vol. 24, pp. 214-227, 2015.
- [24] Ahmed Almradi, "On the Performance of MIMO Full-Duplex Relaying in the Presence of Co-Channel Interference," *Global Communications Conference (GLOBECOM)*, December 2016.
- [25] A.-R. Emilio, W. Stefan, R. López-Valcarce, R. Taneli, and W. Risto, "Wideband Full-Duplex MIMO Relays with Blind Adaptive Self-Interference Cancellation," *Signal Processing*, vol. 130, 2017.
- [26] O. Taghizadeh, J. Zhang, and M. Haardt, "Transmit beamforming aided amplify-and-forward MIMO full-duplex relaying with limited dynamic range," *Signal Processing*, vol. 127, pp. 266-281, 10// 2016.
- [27] N. Bornhorst and M. Pesavento, "Filter-and-forward beamforming with adaptive decoding delays in asynchronous multi-user relay networks," *Signal Process.*, vol. 109, pp. 132-147, 2015.
- [28] S. Huberman and T. Le-Ngoc, "Self-Interference-Threshold-Based MIMO Full-Duplex Precoding," *IEEE Transactions on Vehicular Technology*, vol. 64, pp. 3803-3807, 2015.
- [29] M. Sakai, H. Lin, and K. Yamashita, "Self-interference cancellation in full-duplex wireless with IQ imbalance," *Physical Communication*, vol. 18, Part 1, pp. 2-14, 3// 2016.
- [30] P. Mahecken, T. Riihonen, S. Werner, and R. Wichman, "Constrained Phase Noise Estimation in OFDM Using Scattered Pilots Without Decision Feedback," *IEEE Transactions on Signal Processing*, vol. 65, pp. 2348-2362, 2017.
- [31] Z. Wei, X. Zhu, S. Sun, Y. Huang, L. Dong, and Y. Jiang, "Full-Duplex Versus Half-Duplex Amplify-and-Forward Relaying: Which is More Energy Efficient in 60-GHz Dual-Hop Indoor Wireless Systems?," *IEEE Journal on Selected Areas in Communications*, vol. 33, pp. 2936-2947, 2015.
- [32] D. Liang, P. Xiao, G. Chen, M. Ghorashi, and R. Tafazolli, "Digital self-interference cancellation for Full-Duplex MIMO systems," in *2015 International Wireless Communications and Mobile Computing Conference (IWCMC)*, pp. 403-407, 2015.
- [33] Y. Sung, J. Ahn, B. Van Nguyen, and K. Kim, "Loop-interference suppression strategies using antenna selection in full-duplex MIMO relays," in *Intelligent Signal Processing and Communications Systems (ISPACS), 2011 International Symposium on*, pp. 1-4, 2011.
- [34] T. Riihonen, S. Werner, and R. Wichman, "Spatial loop interference suppression in full-duplex MIMO relays," in *2009 Conference Record of the Forty-Third Asilomar Conference on Signals, Systems and Computers*, pp. 1508-1512, 2009.

